*Journal of Comparative Neurology*

WILEY

JCN RESEARCH IN SYSTEMS NEUROSCIENCE THE JOURNAL OF COMPARATIVE NEUROLOGY

RESEARCH ARTICLE OPEN ACCESS

# The Complexly Parcellated, Yet Quantitatively Reduced, Orexinergic/Hypocretinergic System of Humans

Illke B. Malungo[1] | Ayanda Ngwenya[1] | Mads F. Bertelsen[2] | Muhammad A. Spocter[1,3] | Thomas C. Thannickal[4,5] | Jerome M. Siegel[4,5] | Paul R. Manger[1]

[1]School of Anatomical Sciences, Faculty of Health Sciences, University of the Witwatersrand Parktown, Johannesburg, Republic of South Africa | [2]Centre for Zoo and Wild Animal Health Copenhagen Zoo, Frederiksberg, Denmark | [3]Department of Anatomy, Des Moines University, Des Moines, Iowa, USA | [4]Department of Psychiatry, School of Medicine, and Brain Research Institute, University of California, Los Angeles, Los Angeles, California, USA | [5]Brain Research Institute, Neurobiology Research, Sepulveda VA Medical Center, Los Angeles, California, USA

**Correspondence:** Paul R. Manger (Paul.Manger@wits.ac.za)

**Received:** 21 November 2024 | **Revised:** 29 January 2025 | **Accepted:** 10 February 2025

**Funding:** This work was supported by the South African National Research Foundation (P.R.M.), the Medical Research Service of the Department of Veterans Affairs and R01-DA058639 (T.C.T., J.M.S.), and the Carnegie Corporation of New York (M.A.S., P.R.M.).

**Keywords:** hypocretin | immunohistochemistry | monkey | orexin | primates | RRID:AB_91545 | stereology

## ABSTRACT

The phylogenetic contextualization of human neuroanatomy is crucial for understanding the positive, neutral, and/or negative effects of therapeutic interventions derived from animal models. Here we determined the parcellation of, and quantified, orexinergic (or hypocretinergic) neurons in the hypothalami of humans and several species of primates, including strepsirrhines (two species), platyrrhines (two species), cercopithecoids (three species), and hominoids (three species, including humans). The strepsirrhines, platyrrhines, and cercopithecoids presented with three distinct clusters of orexinergic neurons, revealing an organization like that observed in most mammals. In the three hominoids, an additional orexinergic cluster was found in the tuberal region of the hypothalamus, termed the optic tract cluster extension. In humans only, an additional parvocellular cluster of orexinergic neurons was observed in the dorsomedial hypothalamus. The human presented with the most complex parcellation of orexinergic neurons of the primates studied. Total numbers of orexinergic neurons in nonhuman primates were strongly correlated to brain mass ($P_{uncorr} = 1.2 \times 10^{-6}$), with every doubling in brain mass leading to an ~1.5-times increase in neuron number. In contrast, humans have approximately 74,300 orexinergic neurons, which is significantly less than the 205,000 predicted using the nonhuman primate regression for a brain mass of ~1363 g. We conclude that although the human orexinergic system is the most complex of primates in terms of parcellation, with potential associated functional specializations, this system is quantitatively paradoxical in having a significantly lower neuronal number than expected for a primate with an ~1363-g brain.

**Abbreviations:** 3V, third ventricle; A, amygdaloid complex; ac, anterior commissure; DBH, diagonal band of Broca, horizontal limb; DT, dorsal thalamus; f, fornix; GPi, internal globus pallidus; H, hippocampal formation; Hyp, hypothalamus; ic, internal capsule; itp, inferior thalamic peduncle; MB, mammillary bodies; Mc, main orexinergic cluster; mmt, mammillothalamic tract; N.Bas, nucleus basalis; OC, optic chiasm; OT, optic tract; OTc, optic tract orexinergic cluster; OTce, optic tract orexinergic cluster extension; PC, cerebral peduncle; Pvc, parvocellular orexinergic cluster; PVH, paraventricular hypothalamic nucleus; R, thalamic reticular nucleus; SCN, suprachiasmatic nucleus; SI, substantia innominata; SNR, substantia nigra, reticular part; SON, supraoptic nucleus; STN, subthalamic nucleus; VM, ventromedial hypothalamic nucleus; zi, zona incerta; Zic, zona incerta orexinergic cluster.

## 1 | Introduction

Although increasingly recognized as being involved in many different functions (e.g., Zhang et al. 2013; Kukkonen et al. 2002), the orexinergic (hypocretinergic) system, through the release of the orexin A and B peptides throughout the brain, is involved in: (1) the maintenance of wakefulness and the regulation of the sleep/wake cycle (e.g., Volkhoff 2012; Inutsuka and Yamanaka 2013); (2) the repression of the neural circuits controlling satiety, thus stimulating the intake of food (e.g., Kukkonen et al. 2002; Zhang et al. 2013; Soya and Sakurai 2020); and (3) the mediation of arousal during pleasurable activities, or the reward system (Tsujino and Sakurai 2009; McGregor et al. 2011; Blouin et al. 2013; Siegel 2022; McGregor et al. 2023, 2024). In this sense, the orexinergic system appears to manage a crucial balance between the biological imperatives of the need to obtain nutrition and sleep and the pleasure experienced when these needs are met.

In mammals, orexinergic neurons are primarily restricted to the hypothalamus, although the occasional neuron is observed in the dorsally adjacent zona incerta (e.g., Calvey, Patzke et al. 2015; Williams et al. 2022; Oddes et al. 2023). Mammalian orexinergic neurons are typically organized into three clusters: the main cluster (Mc) in the perifornical region of the hypothalamus; the zona incerta cluster (Zic) in the dorsolateral aspect of the hypothalamus; and the optic tract cluster (OTc) in the ventrolateral aspect of the hypothalamus (e.g., Nixon and Smale 2007; Oddes et al. 2023). Despite this consistency, variations in the nuclear parcellation of the orexinergic system in mammals have been described. One example is the addition of the medially located parvocellular orexinergic cluster in Cetartiodactyla (Dell et al. 2012, Dell, Karlsson et al. 2016; Dell, Patzke et al. 2016; Davimes et al. 2017; Malungo et al. 2020), African elephants (Maseko et al. 2013), lions, and cheetahs (Oddes et al. 2023).

In primates, the distribution and parcellation of the orexinergic neurons have been described in one species of Lorisiformes (Demidoff's dwarf bushbaby), one species of Lemuriforme (ring-tailed lemur) (Calvey, Patzke et al. 2015), and three species of Hominoidea: lar gibbon, chimpanzee (Williams et al. 2022), and human (Elias et al. 1998; Moore et al. 2001;, Thannickal, Moore et al. 2000, Thannickal et al. 2009, 2018). Although the presence of orexinergic neurons in the hypothalamus of the rhesus monkey (*Macaca mulatta*) has been quantified (Downs et al. 2007; Luna et al. 2017), no detailed parcellations of the orexinergic neurons in the hypothalamus of the Platyrrhini, Colobinae, or Cercopithecinae have been presented. In the lar gibbon and chimpanzee, an extension of the optic tract orexinergic cluster into the tuberal region in the anterior ventromedial aspect of the hypothalamus was noted (Williams et al. 2022). In humans, expression of the orexin mRNA was found in this region (Krolewski et al. 2010), but orexinergic neurons were not reported with immunohistochemical staining (Thannickal, Moore et al. 2000). Here we reanalyzed the parcellation and number of orexinergic neurons in the hypothalami of three humans (Thannickal, Moore et al. 2000), two prosimians (Calvey, Patzke et al. 2015), two Platyrrhini (black-capped squirrel monkey, tufted capuchin), and three Cercopithecinae (vervet monkey, crested macaque, olive baboon) to determine potential evolutionary trends in this system.

## 2 | Materials and Methods

### 2.1 | Human Specimens

The three human samples examined in this study include a 44-year-old female (brain mass estimate of 1395 g, A05-25, cause of death breast cancer), a 71-year-old male (brain mass estimate of 1360 g, A18-05, cause of death myocardial infarction), and an 83-year-old female (brain mass estimate of 1325 g, A95-220, cause of death cirrhosis and sepsis) (see Thannickal, Moore et al. 2000, 2018 for full details of procurement of these human tissue samples). These control human hypothalami were sectioned in a coronal plane (40 μm section thickness, with every 12th section being stained for the 44-year-old female and 71-year-old male, and every 6th section being stained for the 83-year-old female). The sections were treated with 0.5% sodium borohydride in phosphate-buffered saline (PBS) for 30 min, washed with PBS, and then incubated for 30 min in 0.5% $H_2O_2$ to block endogenous peroxidase activity. For antigen retrieval, the sections were heated for 30 min at 80°C in a water bath with 10 mM sodium citrate (pH 8.5) solution. The sections were then cooled to room temperature in sodium citrate and washed with PBS. After thorough washing with PBS, the sections were placed for 2 h in 1.5% normal goat serum in PBS and incubated for 72 h at 4°C with a 1:10,000 dilution of Hcrt-1 antibody (Rabbit anti-orexin-A, H-003-30, Phoenix Pharmaceuticals Inc) (see Thannickal, Moore et al. 2000, 2018 for full details of histological processing of these human tissue samples). Sections were then incubated in a secondary antibody (biotinylated goat anti-rabbit IgG, Vector Laboratories), followed by immersion in avidin–biotin–peroxidase complex solution (ABC Elite Kit, Vector Laboratories), for 2 h each at room temperature. The tissue-bound peroxidase was visualized by a diaminobenzidine (DAB) reaction (Vector Laboratories).

### 2.2 | Nonhuman Primate Specimens

In addition to the two Strepsirrhini and the two Hominoidea previously sectioned and analyzed (Calvey, Patzke et al. 2015; Williams et al. 2022), brains were obtained from adult (animals of breeding age, but not senescent) males from two Platyrrhini, including one black-capped squirrel monkey (*Saimiri boliviensis*), one tufted capuchin (*Cebus apella*), and three Cercopithecoidea, including one vervet monkey (*Chlorocebus pygerythrus*), one crested macaque (*Macaca nigra*), and one olive baboon (*Papio anubis*). These primate specimens were acquired from three Scandinavian zoos, were all born at the zoos, and were observed by keepers and veterinary staff throughout their lives. No behavioral problems or stereotypies were observed in any of the primates used in the current study. These primates were treated according to the guidelines of the University of Witwatersrand Animal Ethics Committee (Clearance number 2017/010/73/O), which correspond with those of the NIH for care and use of animals in scientific experimentation. The brains were obtained after the animals had been euthanized with sodium pentobarbital (i.v.), in line with population management decisions of the zoos independent of the current study (Bertelsen 2018). Following euthanasia, the carotid arteries were cannulated, and the heads were perfused with an initial rinse of 0.9% saline solution at a temperature of 4°C followed by 4% paraformaldehyde in 0.1 M phosphate buffer (PB) at 4°C. The brains, which showed no signs

of neuropathology, were removed from the skull and postfixed in 4% paraformaldehyde in 0.1 M PB (48 h at 4°C) and allowed to equilibrate in 30% sucrose in 0.1 M PB before being stored in an antifreeze solution (containing glycerol, ethylene glycol, and PB) at −20°C until use (Manger et al. 2009).

### 2.3 | Sectioning and Immunohistochemical Staining—Nonhuman Primates

Blocks containing the hypothalamus were dissected from these brains, allowed to equilibrate in 30% sucrose in 0.1 M PB, and then frozen in crushed dry ice. The frozen brain blocks were mounted to an aluminum stage, and coronal sections of 50 μm thickness were cut using a sliding microtome. All brain blocks were sectioned in a coronal plane with the 1st section stained for Nissl, the 2nd section immunostained for orexin-A, and then every 10th subsequent section being stained for Nissl (sections 11, 21, 31, etc.) or orexin-A (sections 12, 22, 32, etc.). Sections used for Nissl staining were mounted on 0.5% gelatine-coated glass slides, cleared in a solution of 1:1 chloroform and 100% ethanol overnight, after which the sections were stained with 1% cresyl violet. The Nissl-stained sections were used to define the cytoarchitectural borders of the hypothalamus and adjacent structures.

The series of sections used for orexin-A immunohistochemistry were initially treated for 30 min with an endogenous peroxidase inhibitor (49.2% methanol: 49.2% 0.1 M PB: 1.6% of 30% $H_2O_2$), followed by three 10 min rinses in 0.1 M PB. The sections were then preincubated at room temperature for 3 h in a blocking buffer solution comprising 3% normal goat serum, 2% bovine serum albumin (BSA, Sigma), and 0.25% Triton X-100 (Merck) in 0.1 M PB. The sections were then placed in a primary antibody solution (blocking buffer with appropriately diluted primary antibody) and incubated at 4°C for 48 h under gentle shaking. To identify orexin-A-containing cells bodies, we used the AB3704 anti-orexin-A rabbit polyclonal antibody from Merck-Millipore (AB3704, Merck-Millipore; RRID AB_91545; raised against a synthetic peptide corresponding to the c-terminal portion of bovine orexin-A peptide) at a dilution of 1:3000. The pattern of staining of orexinergic neurons in the hypothalamus was generally like that seen in previously studied primate species (Elias et al. 1998; Moore et al. 2001; Thannickal, Moore et al. 2000, 2009, 2018; Calvey, Patzke et al. 2015; Williams et al. 2022).

The incubation in the primary antibody solution was followed by three 10 min rinses in 0.1 M PB, after which the sections were incubated in a secondary anti-rabbit antibody solution for 2 h at room temperature. The secondary antibody solution contained a 1:1000 dilution of biotinylated anti-rabbit IgG (BA-1000, Vector Labs) in a solution containing 3% NGS and 2% BSA in 0.1 M PB. This was followed by three 10 min rinses in 0.1 M PB after which the sections were incubated in a solution of 0.8% Reactive A plus 0.8% Reactive B in 0.1 M PB (Vectastain Elite ABC-HRP, avidin-biotin complex-horseradish peroxidase, Kit, Peroxidase, PK-7200, Vector Laboratories) for 1 h. After three further 10 min rinses in 0.1 M PB, the sections were placed in a solution of 0.05% DAB in 0.1 M PB for 5 min, followed by the addition of 3 μL of 30% $H_2O_2$ to each 1 mL of solution in which each section was immersed. Chromatic precipitation of the sections was monitored visually under a low-power stereomicroscope. This process was allowed to continue until the background staining of the sections was appropriate for architectonic analysis without obscuring any immunopositive structures. The precipitation process was stopped by immersing the sections in 0.1 M PB and then rinsing them twice more in 0.1 M PB. To check for nonspecific staining from the immunohistochemistry protocol, we omitted either the primary antibody or the secondary antibody, but not both, in selected sections, which produced no evident staining. The immunohistochemically stained sections were mounted on 0.5% gelatine-coated slides and left to dry overnight. The sections were then dehydrated in graded series of ethanol, cleared in xylene, and cover slipped with Depex.

### 2.4 | Anatomical Reconstruction, Microphotography, and Nomenclature

A low-power stereomicroscope was used to examine the Nissl-stained sections and camera lucida drawings outlining architectural borders were made. The associated orexin-A-immunostained sections were matched to these drawings, and the stained neurons were marked. The drawings were then scanned and redrawn using the Canvas X Draw program (Canvas GFX Inc., FL, USA). Digital photomicrographs were captured using an Axiocam 208 color camera mounted to a Zeiss Axioskop microscope (with Zeiss A-Plan 5x/012, Zeiss Plan-NeoFluar 10x/0.30, and Zeiss Plan-NeoFluar 40x/0.75 objectives). No pixilation adjustments or manipulation of the captured images were undertaken, except for the adjustment of contrast, brightness, and levels using Adobe Photoshop.

### 2.5 | Stereological Analysis

To quantify the total numbers of orexinergic neurons in the hypothalami of the three human specimens and the five non-human primate species studied herein, as well as those of two strepsirrhine primates previously studied—Demidoff's dwarf bushbaby (*Galago demidoff*) and a ring-tailed lemur (*Lemur catta*) (Calvey, Patzke et al. 2015; part of a histological collection curated by PRM)—an unbiased design-based systematic random sampling stereological protocol was employed. We used an MBF Bioscience (LLC, Williston, VT, USA) system with a three-plane motorized stage, Zeiss.Z2 Axio Imager Vario microscope, and Stereo Investigator software (MBF, version 2018.1.1.1; 64-bit). Initially, pilot studies were conducted to optimize sampling parameters, such as the counting frame and sampling grid sizes, and achieve an appropriate coefficient of error (CE) (Gundersen 1988; West et al. 1991; Dell, Karlsson et al. 2016). In addition, we measured the tissue section thickness at every sampling site. The vertical guard zone, at both the top and bottom of the section, was determined according to tissue thickness to avoid errors/biases due to sectioning artifacts (West et al. 1991; Dell, Karlsson et al. 2016), and stereological counts were undertaken using a 40× objective. Table 1 provides a detailed summary of the stereological parameters employed in the current study, with Table 2 providing the results obtained. To estimate the total number of orexinergic neurons, we used the optical fractionator probe (West et al. 1991; Dell, Karlsson et al. 2016), first estimating the total number within these clusters in the right hypothalamus and then doubling this estimate to obtain the total number of orexinergic neurons.

**TABLE 1** | Stereological parameters used for estimating the number of neurons immunopositive for orexin-A in the primates studied.

| Species | Counting frame size (μm) | Sampling grid size (μm) | Disector height (μm) | Cut thickness (μm) | Average mounted thickness (μm) | Vertical guard zones (top and bottom, μm) | Section interval | Number of sections | Number of sampling sites | Average CE (Gundersen $m = 0$) | Average CE (Gundersen $m = 1$) |
|---|---|---|---|---|---|---|---|---|---|---|---|
| *Galago demidoff* | 200 × 200 | 250 × 250 | 14 | 50 | 12.8 | 2 | 6 | 4 | 158 | 0.26 | 0.07 |
| *Lemur catta* | 200 × 200 | 400 × 400 | 14 | 50 | 14.5 | 2 | 6 | 9 | 410 | 0.06 | 0.05 |
| *Saimiri boliviensis* | 200 × 200 | 400 × 400 | 14 | 50 | 15.0 | 2 | 5 | 12 | 430 | 0.07 | 0.05 |
| *Cebus apella* | 200 × 200 | 400 × 400 | 14 | 50 | 13.8 | 2 | 5 | 20 | 1063 | 0.05 | 0.03 |
| *Chlorocebus pygerythrus* | 200 × 200 | 400 × 400 | 14 | 50 | 13.8 | 2 | 5 | 17 | 835 | 0.06 | 0.04 |
| *Macaca nigra* | 200 × 200 | 400 × 400 | 14 | 50 | 13.4 | 2 | 5 | 21 | 1898 | 0.04 | 0.03 |
| *Papio anubis* | 200 × 200 | 400 × 400 | 14 | 50 | 16.4 | 2 | 5 | 18 | 1801 | 0.03 | 0.03 |
| *Homo sapiens (F 44)* | 200 × 200 | 400 × 400 | 14 | 40 | 15.7 | 2 | 12 | 18 | 3466 | 0.05 | 0.03 |
| *Homo sapiens (F 83)* | 250 × 250 | 400 × 400 | 14 | 40 | 12.9 | 2 | 6 | 43 | 7677 | 0.03 | 0.02 |
| *Homo sapiens (M 71)* | 200 × 200 | 400 × 400 | 14 | 40 | 13.2 | 2 | 12 | 19 | 4073 | 0.15 | 0.04 |

**TABLE 2** | Brain mass, total numbers of orexinergic neurons (both left and right hypothalamus), and cell volumes determined in the primate examined in the current study and from previous reports in the literature.

| Scientific name | Common name | Brain mass (g) | Total number (mean section thickness) | Range of total number | Cell volume ($\mu m^3$) | Source |
|---|---|---|---|---|---|---|
| *Galago demidoff* | Demidoff's dwarf bushbaby ($n = 1$) | 3.5 | 7497 | — | 2858 | 1, 2 |
| *Lemur catta* | Ring-tailed lemur ($n = 1$) | 24.1 | 19,246 | — | 2745 | 1, 2 |
| *Saimiri boliviensis* | Black-capped squirrel monkey ($n = 1$) | 26.1 | 20,562 | — | 3121 | 2 |
| *Cebus paella* | Tufted capuchin ($n = 1$) | 66.1 | 34,692 | — | 3096 | 2 |
| *Chlorocebus pygerythrus* | Vervet monkey ($n = 1$) | 71.8 | 28,857 | — | 2519 | 2 |
| *Macaca nigra* | Crested macaque ($n = 1$) | 91.3 | 52,924 | — | 3442 | 2 |
| *Papio anubis* | Olive baboon ($n = 1$) | 146.6 | 57,101 | — | 4045 | 2 |
| *Hylobates lar* | Lar gibbon ($n = 1$) | 112.0 | 52,567 | — | 4664 | 3 |
| *Pan troglodytes* | Chimpanzee ($n = 1$) | 388.1 | 107,396 | — | 5926 | 3 |
| *Homo sapiens* | Human ($n = 1$—F 44) | 1375–1415 | 113,101 | — | Mc—8454 Pvc—3271 | 2 |
| *Homo sapiens* | Human ($n = 1$—M 71) | 1325–1400 | 126,252 | — | Mc—7224 Pvc—2201 | 2 |
| *Homo sapiens* | Human ($n = 1$—F 83) | 1300–1350 | 76,511 | — | Mc—6556 Pvc—1995 | 2 |
| *Homo sapiens* | Human ($n = 7$, control specimens only) | 1400 | 74,329 | 61,050–79,575 | n.d. | 4 |
| *Homo sapiens* | Human ($n = 8$, control specimens only) | 1340.5 | 83,188 | 54,900–127,300 | n.d. | 5 |
| *Homo sapiens* | Human ($n = 9$, control specimens only) | 1400 | 36,842 | 17,400–65,900 | n.d. | 6 |
| *Homo sapiens* | Human ($n = 10$, control specimens only) | 1279.4 | 21,310 | 10,700–33,000 | n.d. | 7 |
| *Homo sapiens* | Human ($n = 12$, control specimens only) | 1400 | 62,754 | 50,804–82,511 | n.d. | 8 |

*Note:* Sources of data: 1—Calvey, Patzke et al. (2015); 2—This study; 3—Williams et al. (2022); 4—Thannickal et al. (2000); 5—Fronczek et al. (2005); 6—Fronczek et al. (2007); 7—Fronczek et al. (2012); 8—Valko et al. (2013) number is the average of control subjects 1–12.
Abbreviations: Mc, cell volumes in main cluster of human; n.d., no available data; Pvc, cell volumes in parvocellular cluster of humans.

To determine orexinergic neuronal volumes, we used the nucleator probe, with five rays being sampled in each probe. For all nonhuman primate tissues without data in the literature, sampling with this probe was used concurrently with the optical fractionator while maintaining strict criteria, that is, only neurons with complete cell bodies were analyzed. This resulted in several hundred soma volumes estimated in each species. For the three humans specimens analyzed, in excess of 100 cell volumes from both the Mc and the parvocellular cluster (Pvc) were determined with the nucleator probe for each specimen.

### 2.6 | Statistical Analysis

Using phylogenetic generalized least squares (PGLS) regression analysis, we quantitatively compared the bivariate relationships of brain mass against the orexinergic cell parameters (i.e., total count and soma volume). All statistical analyses were performed on logarithmically transformed (base 10) data and were implemented in R Version 4.01 (http://www.r-project.org/, RRID:SCR_001905). PGLS statistics were computed using the "EvoMap" add-on package (Smaers and Rohlf 2016) in combination with the "caper" add-on package (Orme et al. 2013). The phylogeny used in the current study was derived from Arnold et al. (2010). A summary of the regression statistics derived from these analyses is provided in Table 3. Significance testing for differences in mean cell volume between the main and Pvcs was performed using a Mann–Whitney *U*-test.

## 3 | Results

The current study provides a detailed description of the parcellation and quantification of orexinergic neurons within the

**TABLE 3** | Summary of the regression statistics of orexin number and volume scaled against brain mass in Primates (see Table 2).

| Model (*x* variable; *y* variable) | $\lambda$ | Multiple $R^2$ | Adjusted $R^2$ | Slope | SE | *t* value | *p* | Intercept | SE | *t* value | *p* |
|---|---|---|---|---|---|---|---|---|---|---|---|
| PGLS (brain mass; orexin neuron number) | 0 | 0.971 | 0.967 | 0.571 | 0.037 | 15.32 | $1.22 \times 10^{-6}$ | 3.521 | 0.069 | 51.34 | $2.79 \times 10^{-10}$ |
| PGLS (brain mass; orexin cell volume) | 0 | 0.496 | 0.426 | 0.145 | 0.055 | 2.62 | 0.0343 | 3.286 | 0.102 | 32.24 | $7.14 \times 10^{-9}$ |

Abbreviations: Regression statistics were obtained using phylogenetic generalized least squares regression analysis (PGLS). PGLS was performed using Caper (Orme et al. 2013) and EvoMaps (Smaers and Rohlf 2016).

hypothalamus of primates from across the radiation. Our analysis indicates that although there are significant similarities in terms of clustering of orexinergic neurons across species, in the Hominoids (lar gibbon, chimpanzee, and human), there is an additional cluster, termed the OTc extension (OTce) (Williams et al. 2022), located in the ventromedial hypothalamus. In the human, another additional distinct cluster of orexinergic neurons with small soma, termed the Pvc, was noted in the medial hypothalamus. Stereological analyses indicate that across the nonhuman primates, there is a distinct, and statistically significant, negative allometry of orexinergic neuron numbers with brain mass. Paradoxically, the number of orexinergic neurons in the human specimens appears to be significantly lower than would be predicted based on the allometric relationship determined in nonhuman primates.

### 3.1 | Parcellation of Orexinergic Neurons in Non-Hominoid Primates

Our observations regarding the distribution and clustering of orexinergic-immunopositive neurons in the seven non-hominoid primates examined revealed three distinct clusters located within the hypothalamus, in agreement with the previous description provided for Demidoff's dwarf bushbaby and the ring-tailed lemur (Calvey, Patzke et al. 2015). The three clusters identified include a Mc, a Zic, and an OTc. In these non-hominoid primates, a moderate-to-high density of bipolar and multipolar orexinergic-immunopositive neurons found in the perifornical region formed a distinct cluster (Figures 1–9). We term this cluster the Mc, and it is distinguished from other clusters based on the perifornical location and that the fact the dendrites emanating from these neurons show no distinct preferential orientation (Figures 5–9).

Extending into the dorsolateral aspect of the hypothalamus, a moderate-to-low density cluster of orexinergic neurons was noted and assigned to the Zic (Figures 1–4). Most of these Zic orexinergic neurons were bipolar, but some were multipolar (Figures 5–9). Although topographically continuous with the orexinergic neurons of the Mc, the orexinergic neurons forming the Zic exhibited dendrites consistently oriented in a plane parallel to the dorsal lateral border of the hypothalamus (Figures 5–9). In all non-hominoid species studied, a small number of the orexinergic neurons of the Zic were located dorsolateral to the gray matter of the hypothalamus, located within the both the gray matter forming the zona incerta and ventrally adjacent white matter (Figures 1–9). Extending from the ventrolateral border of the Mc, a moderate-to-low density of orexinergic neurons was noted in the ventrolateral aspect of the hypothalamus, dorsomedially adjacent to the optic tract, and assigned to the OTc (Figures 1–4). These neurons were primarily bipolar, but some were multipolar (Figures 5–9). While in topographic continuity with the orexinergic neurons of the Mc, the neurons of the OTc exhibited a distinct dorsomedial to ventrolateral orientation of the dendrites (Figures 5–9).

### 3.2 | Parcellation of Orexinergic Neurons in Nonhuman Hominoids

In the two nonhuman hominoids surveyed in the current study, the lar gibbon and chimpanzee, using the sectioned and stained

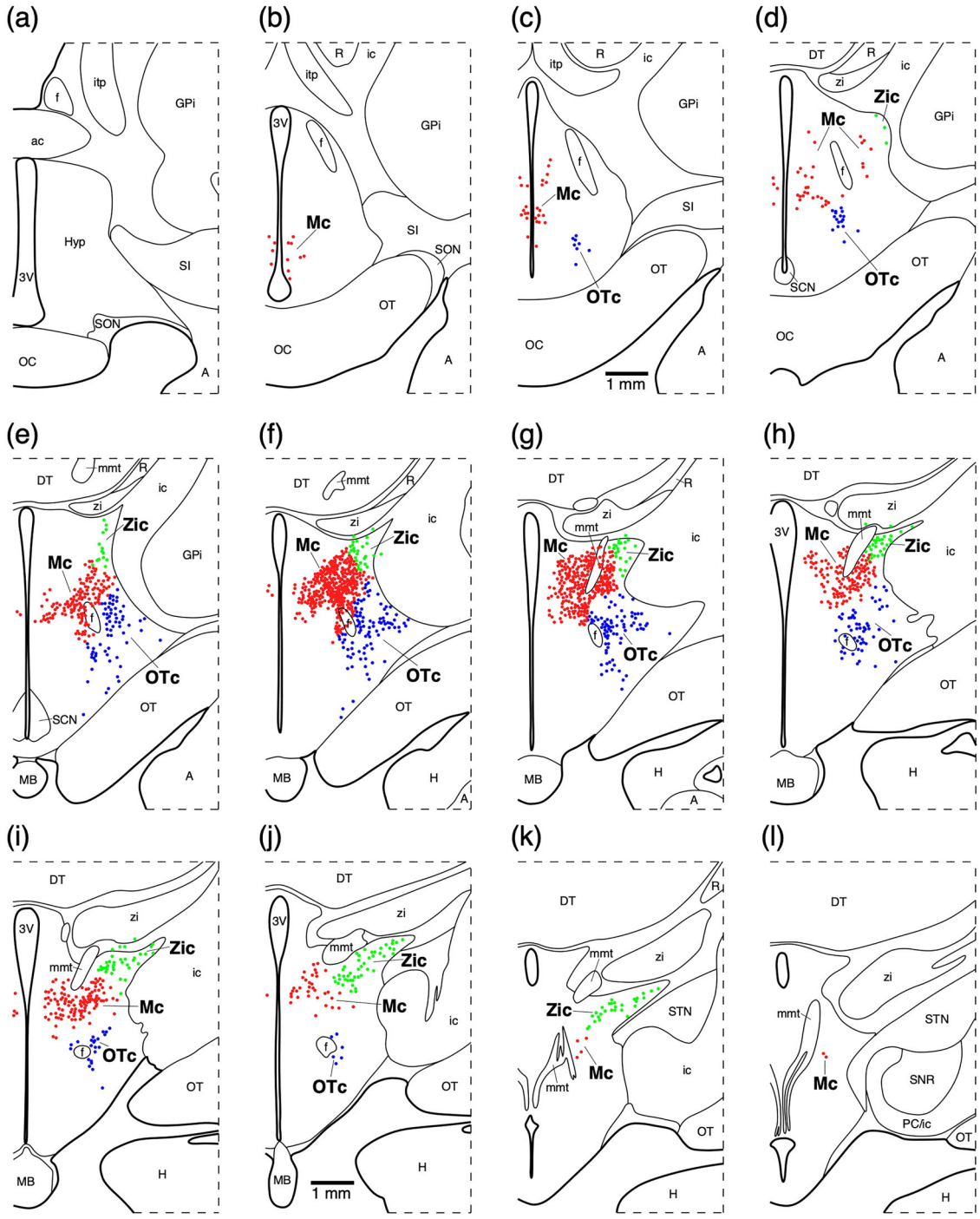


**FIGURE 1** | Serial drawings of coronal sections through one half of a black-capped squirrel monkey (*Saimiri boliviensis*) hypothalamus from the level of the decussation of the anterior commissure (**ac**) to the level of the mammillothalamic tract (**mmt**) showing the distribution of orexin-A immunopositive neurons. Part (a) is the most rostral section, and (l) the most caudal. The outlines of the architectonic regions were drawn using Nissl staining and orexin-A immunoreactive neurons marked on the drawings. Solid red dots represent orexinergic neurons of the main cluster (**Mc**), solid green dots represent orexinergic neurons of the zona incerta cluster (**Zic**), and solid blue dots represent orexinergic neurons of the optic tract cluster (**OTc**). Each dot represents an individual neuron. The individual drawings comprising this figure (a–l) are approximately 250 μm apart, and in each individual, drawing dorsal is to the top and medial to the left. See list for abbreviations.

specimens described in Williams et al. (2022), we noted the same distribution and clustering of orexinergic neurons as described previously (see Williams et al. 2022 for a full description, including distributional mapping of these neurons). In brief, the Mc, Zic, and OTc as described above (Section 3.1) were observed in both species. A low density of orexinergic neurons in the ventromedial aspect of the hypothalamus, in the tuberal region, was noted and assigned to the OTce as reported by Williams et al. (2022).

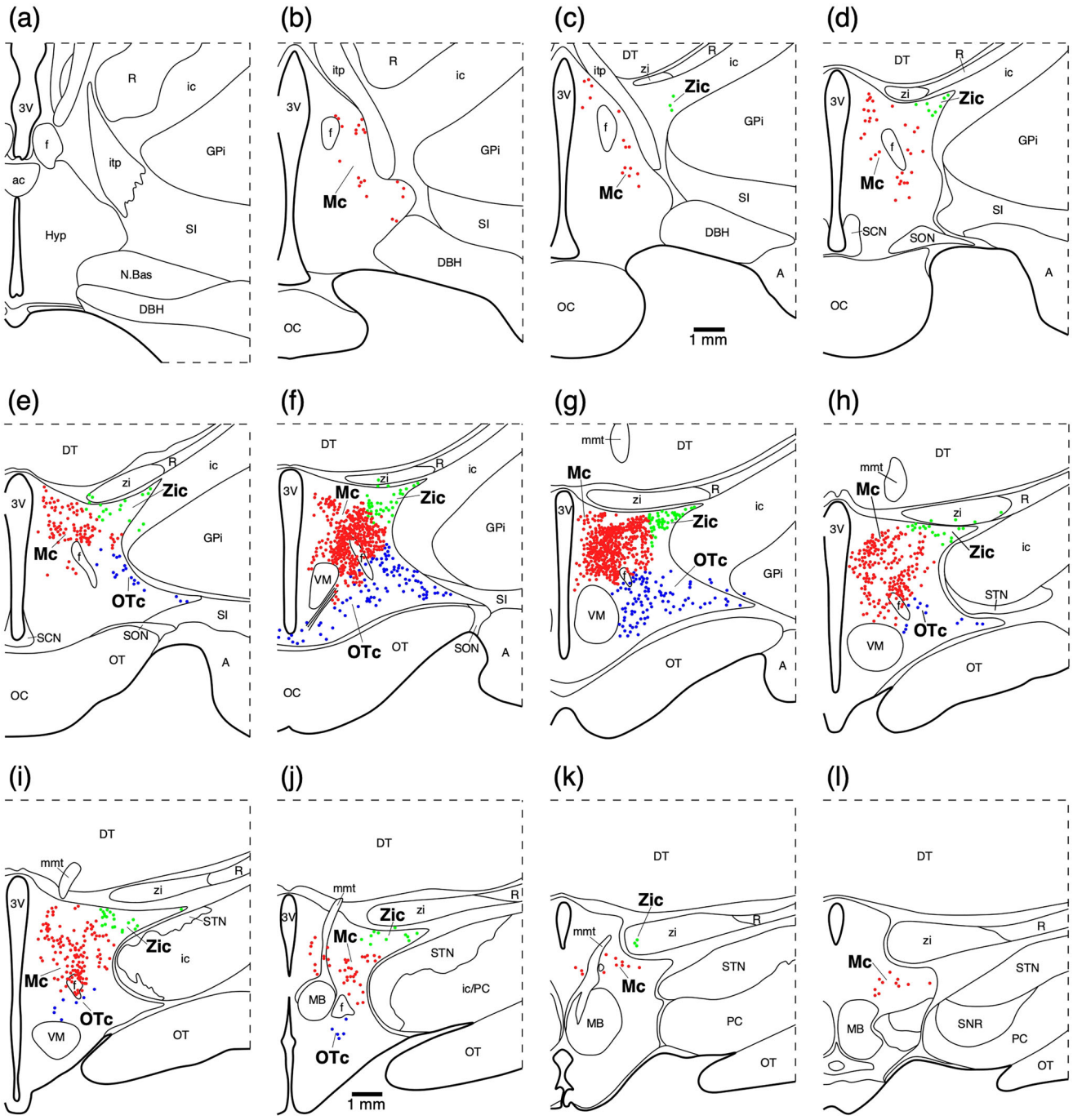


**FIGURE 2** | Serial drawings of coronal sections through one half of a crested macaque (*Macaca nigra*) hypothalamus from the level of the decussation of the anterior commissure (**ac**) to the level of the mammillary bodies (**MB**) showing the distribution of orexin-A immunopositive neurons. Part (a) is the most rostral section, and (l) the most caudal. The outlines of the architectonic regions were drawn using Nissl staining and orexin-A immunoreactive neurons marked on the drawings. Solid red dots represent orexinergic neurons of the main cluster (**Mc**), solid green dots represent orexinergic neurons of the zona incerta cluster (**Zic**), and solid blue dots represent orexinergic neurons of the optic tract cluster (**OTc**). Each dot represents an individual neuron. The individual drawings comprising this figure (a–l) are approximately 500 μm apart, and in each individual, drawing dorsal is to the top and medial to the left. See list for abbreviations.

### 3.3 | Parcellation of Orexinergic Neurons in Humans

The distribution and clustering of orexinergic-immunopositive neurons in the three human samples examined revealed five distinct clusters located within the hypothalamus, these divisions being defined based on location, dendritic orientation, and soma size (Figures 10–14). The clusters identified include a Mc, a Zic, and an OTc as seen in the other primates (see Sections 3.1 and 3.2), with an additional cluster located in the ventromedial aspect of the hypothalamus that we term the OTce as seen in the lar gibbon and chimpanzee (Williams et al. 2022) (see Section 3.2). Another additional cluster was located between the lateral wall of the third ventricle and the Mc that was comprised of orexinergic-

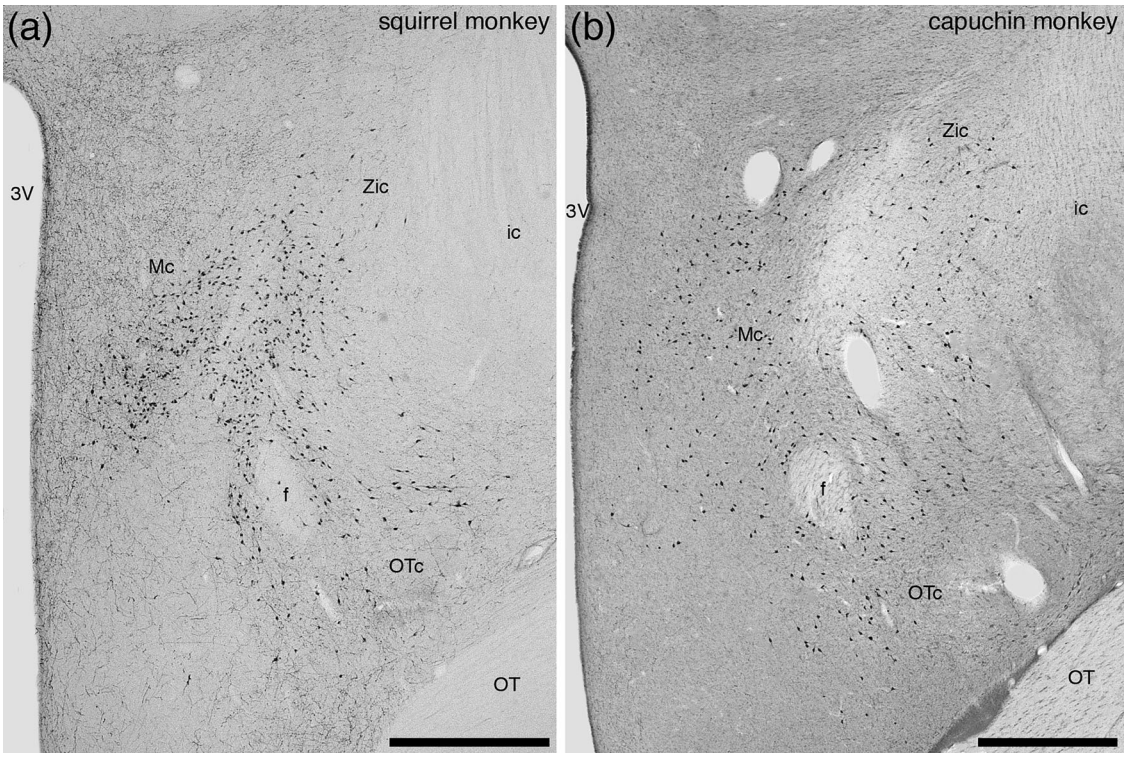


**FIGURE 3** | Low magnification photomicrographs of orexin-A immunopositive neurons at a similar coronal level in the hypothalamus of a black-capped squirrel monkey (a) and a tufted capuchin (b). In both species, the orexin-A immunopositive neurons could be subdivided into main (**Mc**), zona incerta (**Zic**), and optic tract (**OTc**) clusters. In both images, dorsal is to the top and medial to the left. The image provided in (a) from the black-capped squirrel monkey corresponds to drawing g of Figure 1. The scale bars in each image = 1 mm and apply only to that image. See list for abbreviations.

immunopositive neurons with smaller soma that we term the Pvc as observed in certain other mammals (Dell et al. 2012; Maseko et al. 2013; Oddes et al. 2023).

The Mc was observed to be formed by a moderate-to-high density of bipolar and multipolar orexinergic-immunopositive neurons in the perifornical region (Figures 10, 11, and 12c,d). The Mc was distinguished from other clusters on the basis of the perifornical location and that the dendrites emanating from these neurons show no distinct preferential orientation (Figure 12c,d). In the dorsolateral aspect of the hypothalamus, a moderate-to-low density cluster of mostly bipolar orexinergic neurons was assigned to the Zic (Figures 10, 11, and 12a,b). Although this cluster emerges from the dorsolateral border of the Mc, the orexinergic neurons of the Zic exhibited a consistent distinct dendritic orientation in a plane parallel to the dorsal lateral border of the hypothalamus (Figure 12a,b). A small number of the Zic orexinergic neurons were located dorsolateral to the gray matter of the hypothalamus within the gray matter forming the zona incerta and ventrally adjacent white matter (Figures 10 and 11). A moderate-to-low density of mostly bipolar orexinergic neurons in the ventrolateral aspect of the hypothalamus was assigned to the OTc (Figures 10, 11, and 12e,f). While emerging from the ventrolateral aspect of the Mc, the neurons of the OTc exhibited a distinct dorsomedial to ventrolateral orientation of the dendrites (Figure 12e,f).

As observed in the lar gibbon and chimpanzee (Williams et al. 2022), a low density of orexinergic neurons in the ventromedial aspect of the hypothalamus, the tuberal region, was observed in the human specimens and assigned to the OTce (Figures 10, 11, and 13a,b). The OTce orexinergic neurons appear to be an extension of the neurons forming the OTc, being observed in a location ventral and ventromedial to the fornix (Figure 10b–d), in the tuberal region. Although most of these neurons were bipolar, there was a small proportion of neurons that were multipolar (Figure 13a,b). The neurons assigned to the OTce exhibited a distinct preference in dendritic orientation, with the dendrites being oriented primarily in a dorsoventral plane (Figure 13a,b).

Between the Mc and the lateral wall of the third ventricle, a distinct moderately dense cluster of orexinergic neurons (Figures 10 and 11) with substantially smaller soma, the parvocellular orexinergic neuronal cluster (Pvc) (Figure 13c–e; see Section 3.5), was noted. These orexinergic Pvc neurons evinced a mixture of both bipolar and multipolar types, with no apparent preferred dendritic orientation (Figure 13c–e). Although located in a position medial to the Mc, the soma of the Pvc neurons did not contact the lateral wall of the third ventricle, nor were there any CSF-contacting projections emanating from these Pvc neurons (Figure 13c).

### 3.4 | Numbers of Orexinergic Neurons in the Primates Studied

PGLS regression analysis was undertaken on the total orexinergic neuronal numbers in the species analyzed (Table 2). PGLS analysis (Table 3) of the nonhuman primates revealed

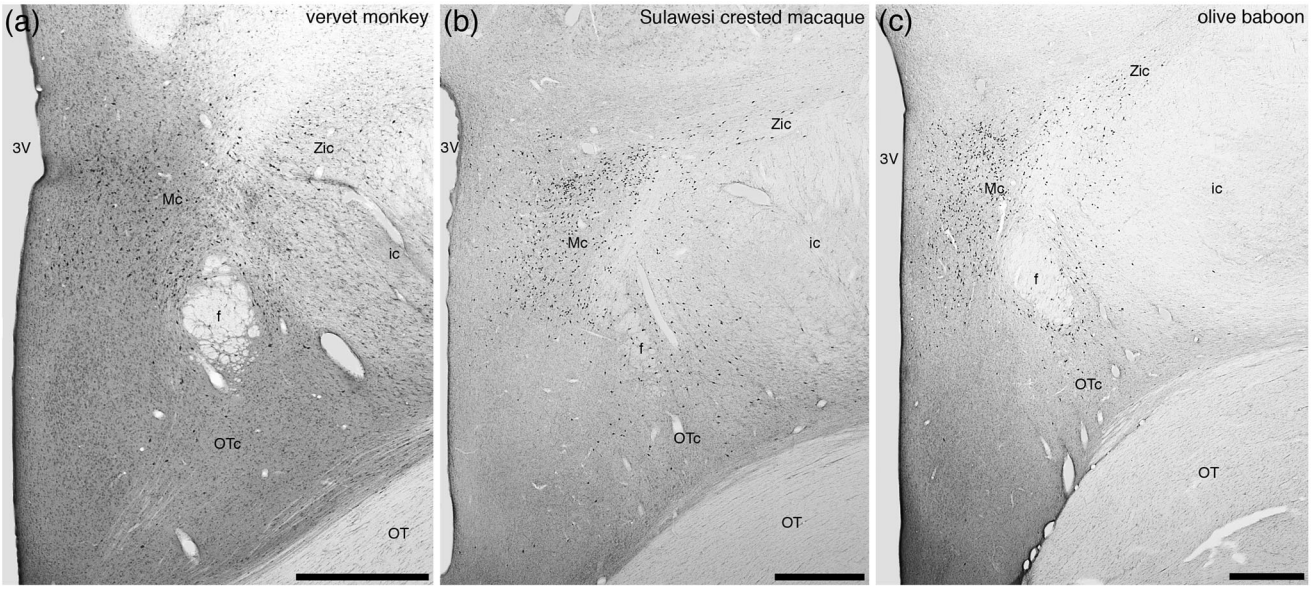


**FIGURE 4** | Low magnification photomicrographs of orexin-A immunopositive neurons at a similar coronal level in the hypothalamus of a vervet monkey (a), a crested macaque (b), and an olive baboon (c). In all three species the orexin-A immunopositive neurons could be subdivided into main (**Mc**), zona incerta (**Zic**), and optic tract (**OTc**) clusters. In all images, dorsal is to the top and medial to the left. The image provided in (b) from the crested macaque corresponds to drawing f of Figure 2. The scale bars in each image = 1 mm and apply only to that image. See list for abbreviations.

no significant phylogenetic signal (lambda [$\lambda$] = 0). A strongly statistically significant negative allometry between orexinergic neuronal number and brain mass was revealed for the nine nonhuman primates studied herein. The number of orexinergic neurons ranged from 7497 in Demidoff's dwarf bushbaby with a brain mass of 3.5 g to 107,396 in the chimpanzee with a brain mass of 388.1 g (Table 2). Regression analysis of brain mass against orexinergic neuron number revealed an allometric regression with a slope of 0.5714, y-intercept of 3315.7, an $R^2$ of 0.9737, and a $P_{\text{uncorr}}$ of $1.2 \times 10^{-6}$ (Figure 14a). Thus, in the nonhuman primates investigated, with every doubling in brain mass, a ~1.5-times (1.486) increase in neuron number was observed, with over 97% of the variance in orexinergic neuronal number being explained by the variance in brain mass.

The data generated in the current study revealed that the total numbers of orexinergic neurons in 3 adult humans were 113,101 (female, 44 years old), 126,252 (male, 71 years old), and 76,511 (female, 83 years old) (Table 2). These data are comparable with previously published work on humans considered "controls," where total orexinergic neuronal numbers ranged from 10,700 to 127,300 (Table 2). Combining all data on human orexinergic neuronal numbers reveals an average number of 74,286. We compared the data on total orexinergic neuronal numbers generated in the current study along with data gleaned from the literature (Table 2) to the statistically significant allometric data derived from nonhuman primates (Figure 14a). In all cases, the numbers of orexinergic neurons reported for humans fall below both the 95% prediction and confidence intervals for the regression derived from nonhuman primates (Figure 14a). This indicates that humans have a considerably lower number of orexinergic neurons than would be predicted for a primate with a brain mass averaging ~1363 g.

### 3.5 | Soma Volumes of Orexinergic Neurons in the Primates Studied

PGLS regression analyses were undertaken on the soma volumes in the species analyzed (Table 2). PGLS analysis (Table 3) of the nonhuman primates revealed no significant phylogenetic signal (lambda [$\lambda$] = 0). The soma volumes of the orexinergic neurons in the nonhuman primates ranged from 2519 $\mu m^3$ in the vervet monkey with a brain mass of 71.8 g to 5926 $\mu m^3$ in the chimpanzee with a brain mass of 388.1 g (Table 2). A statistically significant ($P_{\text{uncorr}}$ = 0.03) negative allometric relationship between orexinergic soma volume and brain mass was revealed for the nine nonhuman primates studied herein (slope = 0.1454, y-intercept = 1930.7, $R^2$ of 0.5947), such that for every doubling in brain mass, the volume of the soma increased by ~1.1 (1.106) times, with ~59.5% of the variation in soma volume explained by variance in brain mass (Figure 14b).

As identified qualitatively (see Section 3.3), the orexinergic system of humans can be parcellated into five clusters. Of these clusters, the neurons of the Pvc appeared to be substantially smaller than those forming the remaining four clusters. Soma volumes in humans were determined for 388 neurons in the Mc and 410 neurons from the Pvc in the three specimens analyzed (Table 2). When grouped, the average somal volume of a human orexinergic neuron located within the Mc was 7375 $\mu m^3$ ($SD$ = 2569 $\mu m^3$). The average somal volume of a human orexinergic neuron located within the Pvc was 2434 $\mu m^3$ ($SD$ = 964 $\mu m^3$). The somal volumes of the Pvc neurons were statistically significantly smaller than those of the Mc in each individual human ($p < 0.001$ in each specimen) (Figure 14b–e). When compared to the regression analysis undertaken for the nonhuman primates, the orexinergic soma volumes exhibit two interesting features. First, the human Mc soma volumes fall

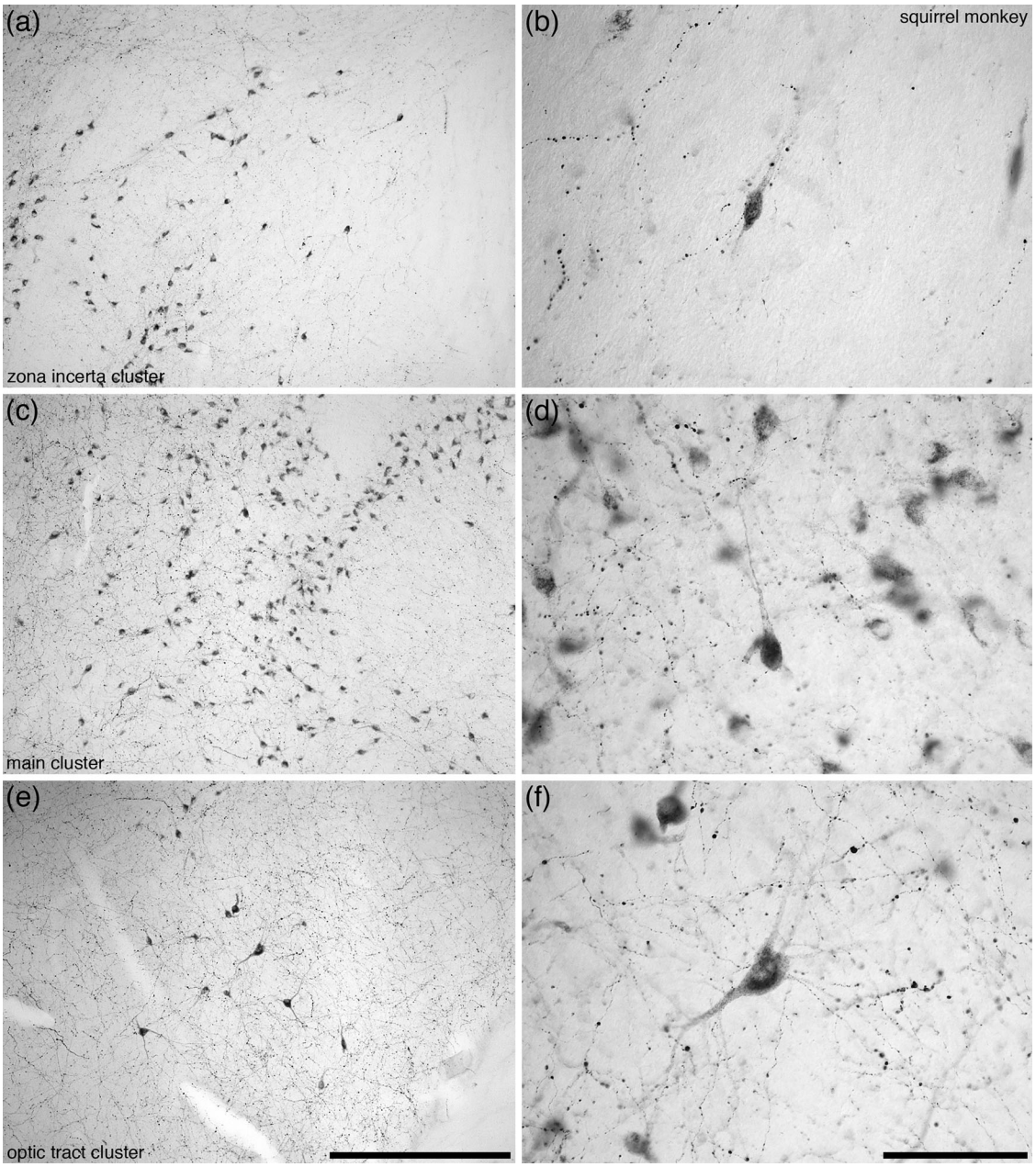


**FIGURE 5** | Moderate (a, c, e) and higher (b, d, f) magnification photomicrographs of orexin-A immunopositive neurons in the hypothalamus of a black-capped squirrel monkey. Parts (a) and (b) depict orexinergic neurons of the zona incerta cluster, (c) and (d) orexinergic neurons of the main cluster, and (e) and (f) orexinergic neurons of the optic tract cluster. In all images, dorsal is to the top and medial to the left. Scale bar in (e) = 500 μm and applies to (a), (c), and (e). Scale bar in (f) = 100 μm and applies to (b), (d), and (f).

within the 95% confidence intervals derived from the nonhuman primate regression, indicating that they are within the range of volumes to be expected for a primate with a brain mass of ~1363 g; however, it should be noted that they are on the larger end of the expected range (Figure 14b). On the basis of the nonhuman primate regression, the soma volume of the human Mc neurons should be approximately 5514 $\mu m^3$, indicating that in humans the Mc neurons are somewhat larger than would be expected for a primate with a brain mass of ~1363 g. In contrast, the human Pvc soma volumes fall below the 95% prediction interval derived from the nonhuman primate regression, reaffirming their small size and novel appearance within humans (Figure 14b).

### 3.6 | Orexinergic Axonal Terminal Bouton Morphology in Primates

In a range of previously studied species, including 10 cetartiodactyls (Dell et al. 2015), lar gibbon and chimpanzee (Williams et al. 2022), lions and cheetah (Oddes et al. 2023), and 5 larger brained birds (Mazengenya et al. 2024), it has been noted that within the orexinergic terminal axons, 2 bouton types, larger and smaller, are observed. In the current study, we examined the hypothalamus and adjacent regions in the human sections for orexinergic terminal axons and observed the two bouton types (Figure 15). As observed in other mammalian and avian

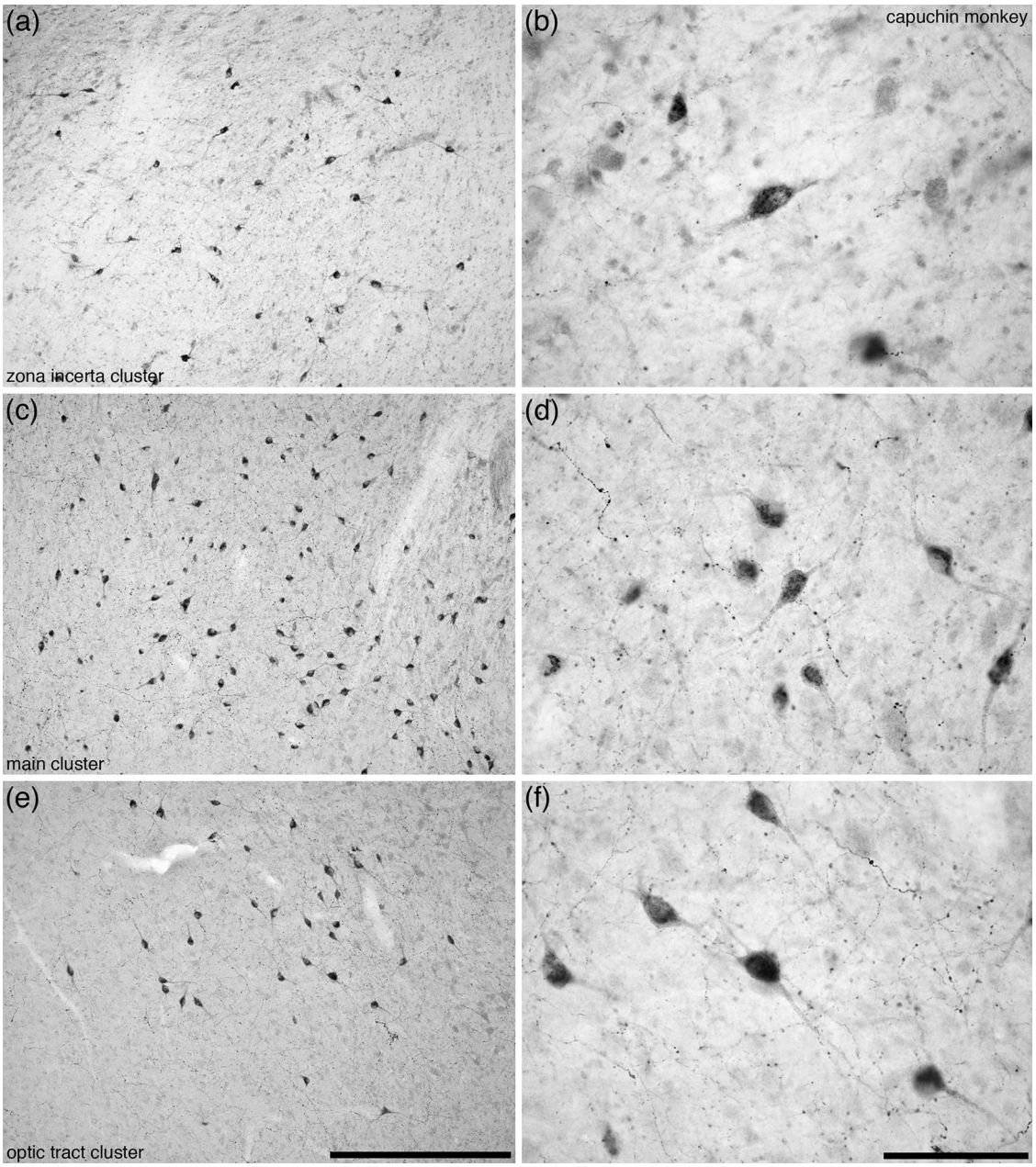


**FIGURE 6** | Moderate (a, c, e) and high (b, d, f) magnification photomicrographs of orexin-A immunopositive neurons in the hypothalamus of a tufted capuchin. Parts (a) and (b) depict orexinergic neurons of the zona incerta cluster, (c) and (d) orexinergic neurons of the main cluster, and (e) and (f) orexinergic neurons of the optic tract cluster. In all images, dorsal is to the top and medial to the left. Scale bar in (e) = 500 μm and applies to (a), (c), and (e). Scale bar in (f) = 100 μm and applies to (b), (d), and (f).

species, the smaller orexinergic boutons substantially outnumber the larger orexinergic boutons.

## 4 | Discussion

The present study describes the parcellation and quantification of the hypothalamic orexinergic neurons of primates, including humans. In all primate species, as observed in all other mammals studied to date (Oddes et al. 2023), the orexinergic neurons were found primarily in the hypothalamus. Like most other mammals, in all primates studied, the Mc, Zic, and OTc of orexinergic neurons were observed. In the hominoids studied herein (lar gibbon, chimpanzee, and human), an additional cluster was observed—the OTce located in the tuberal region of the hypothalamus. In the human only, another additional cluster of orexinergic neurons that we term the Pvc as it comprised neurons with substantially smaller soma was located between the Mc and the lateral wall of the third ventricle. Thus, in terms of the complexity of the parcellation of the orexinergic system, the human presents with the most complex parcellation of the primates studied. Across the nonhuman primates, a distinct and strongly statistically significant negative allometry between brain mass and orexinergic neuronal number was observed.

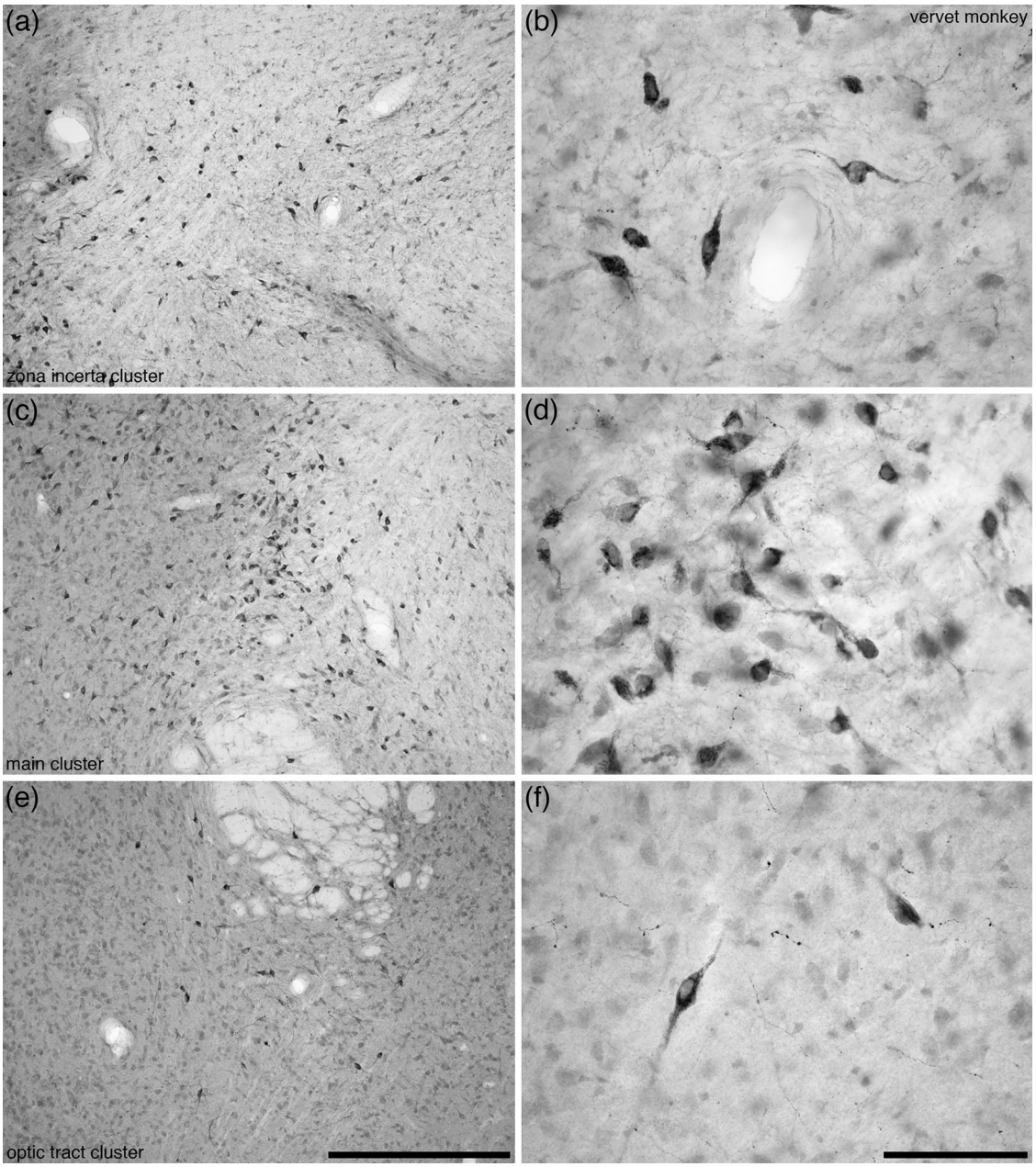


**FIGURE 7** | Moderate (a, c, e) and high (b, d, f) magnification photomicrographs of orexin-A immunopositive neurons in the hypothalamus of a vervet monkey. Parts (a) and (b) depict orexinergic neurons of the zona incerta cluster, (c) and (d) orexinergic neurons of the main cluster, and (e) and (f) orexinergic neurons of the optic tract cluster. In all images, dorsal is to the top and medial to the left. Scale bar in (e) = 500 μm and applies to (a), (c), and (e). Scale bar in (f) = 100 μm and applies to (b), (d), and (f).

Paradoxically, despite having the most complex parcellation, the number of orexinergic neurons in the human hypothalamus was significantly lower than would be expected for a primate of its brain mass. The volume of the orexinergic soma revealed a shallow negative allometry across the nonhuman primates, and the volume of the orexinergic soma in humans, excluding the parvocellular orexinergic neurons, is consistent with this allometry. In addition, we note the presence of both small and large orexinergic boutons on the ramifying orexinergic axonal ramifications. These findings are discussed in an evolutionary and functional context.

### 4.1 | Potential Methodological Issues With Quantification of Human Orexinergic Neurons

That the parcellation of the orexinergic neurons in the human hypothalamus is more complex than seen in all other primates studied is a finding that is comparatively easy to support both conceptually and based on the evidence provided (see Sections 4.2, 4.3, and 4.4). In contrast, the finding that the number of orexinergic neurons in the human hypothalamus is, relative to brain mass, quite small (approximately 74,300 orexinergic neurons, or about 36% of the number predicted using the nonhuman primate

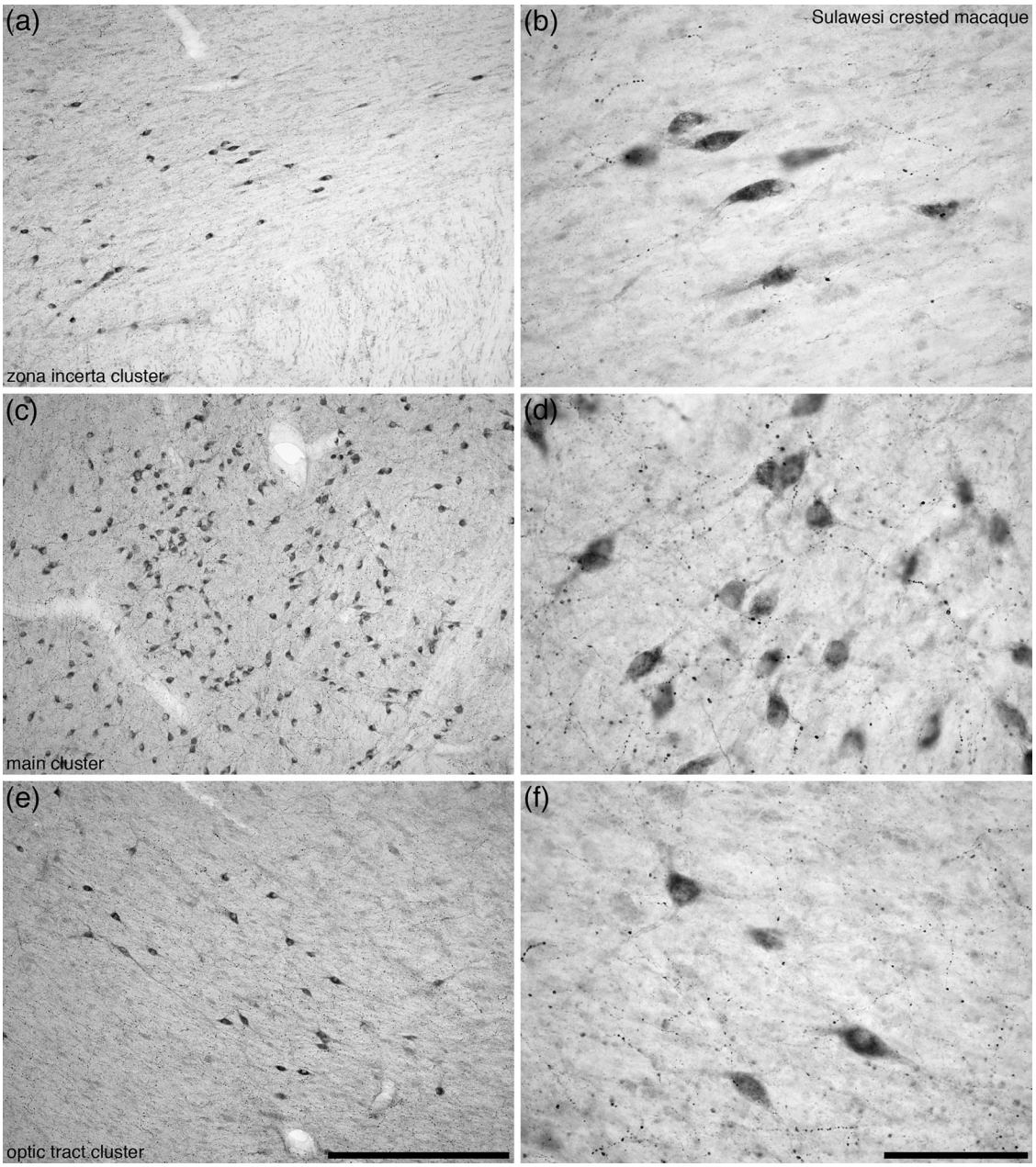


**FIGURE 8** | Moderate (a, c, e) and high (b, d, f) magnification photomicrographs of orexin-A immunopositive neurons in the hypothalamus of a crested macaque. Parts (a) and (b) depict orexinergic neurons of the zona incerta cluster, (c) and (d) orexinergic neurons of the main cluster, and (e) and (f) orexinergic neurons of the optic tract cluster. In all images, dorsal is to the top and medial to the left. Scale bar in (e) = 500 μm and applies to (a), (c), and (e). Scale bar in (f) = 100 μm and applies to (b), (d), and (b).

regression for a brain mass of ~1363 g) may be indicative of methodological issues rather than a reflection of a real difference in the human orexinergic system as compared to other primates.

One of the principal differences between the nonhuman primates and human specimens studied herein is that the nonhuman primates were all healthy adults with no known neurological problems (either behaviorally or when examining the brains postmortem) that were euthanized and the brain immediately perfusion-fixed with 4% paraformaldehyde (Manger et al. 2009), a protocol that cannot be ethically performed on humans. The human tissue examined in this study, and other human studies, was primarily preserved, with variable postmortem intervals and fixation times, in 10% buffered formalin, with this fixation process requiring antigen retrieval procedures during immunohistochemical staining to maximize the revelation of orexinergic neurons (Thannickal, Moore et al. 2000, 2009; Fronczek et al. 2005, 2007, 2012; Valko et al. 2013). A further procedural issue is the different antibodies employed in the different studies, including within this study when comparing the nonhuman primates to the human samples (Thannickal, Moore et al. 2000, 2009; Fronczek et al. 2005, 2007, 2012; Valko et al. 2013). These tissue preparation and staining procedure differences have the potential to reveal a relatively lower number of orexinergic neurons in the human tissue with immunohistochemical techniques when compared to the nonhuman primates studied.

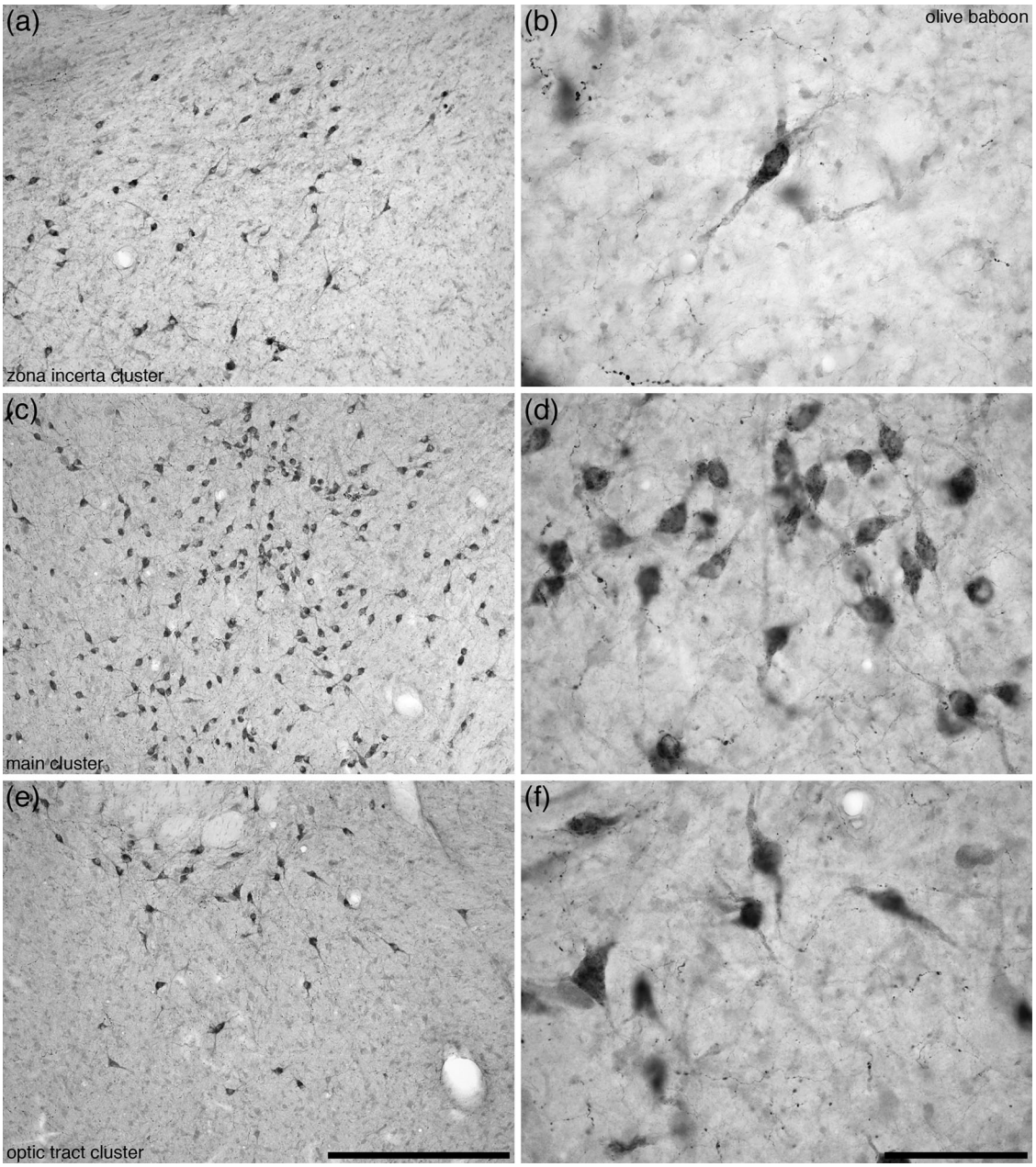


**FIGURE 9** | Moderate (a, c, e) and high (b, d, f) magnification photomicrographs of orexin-A immunopositive neurons in the hypothalamus of an olive baboon. Parts (a) and (b) depict orexinergic neurons of the zona incerta cluster, (c) and (d) orexinergic neurons of the main cluster, and (e) and (f) orexinergic neurons of the optic tract cluster. In all images dorsal is to the top and medial to the left. Scale bar in (e) = 500 μm and applies to (a), (c), and (e). Scale bar in (f) = 100 μm and applies to (b), (d), and (f).

An analytical difference that may result in variations in the estimates of the orexinergic neuronal numbers in humans is the various counting techniques used. To avoid this potential error, we stereologically estimated the number of orexinergic neurons in three human specimens using the same protocol used for the nonhuman primates, using the exact same stereology system (i.e., all original data reported herein regarding neuronal number estimates were determined on the same physical system using the same software). Two previously analyzed human specimens that were reanalyzed in this study reported counts of total orexinergic neurons for the 83-year-old female to be 56,000 (Thannickal, Moore et al. 2000), whereas our estimate was 76,511, and for the 44-year-old female, the total number of orexinergic neurons was previously reported to be 86,354 (Thannickal et al. 2018) with our estimate being 113,101. Thus, our counts are higher than previously reported, but still well below the 205,000 predicted based on the allometry found in nonhuman primates.

Another potential problem that cannot be overcome is that it is likely that the humans, from which the hypothalami were excised and stained, were receiving some type of medication associated with the cause of death (in the three cases studied herein, the patients are likely to have been receiving medication associated with myocardial infarction, breast cancer, cirrhosis, and sepsis). Although it has not been shown that medications associated with these ailments affect the number of neurons

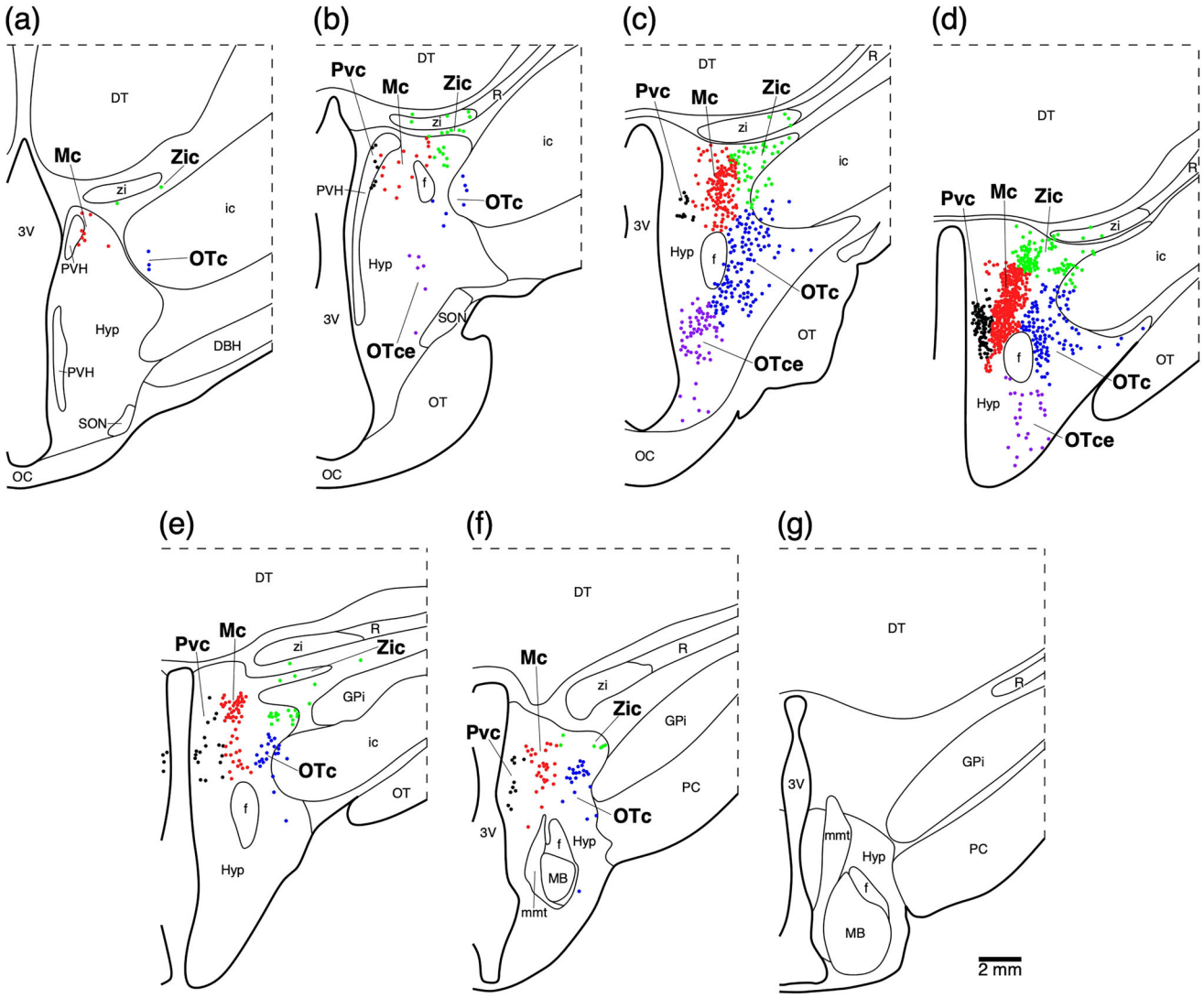


**FIGURE 10** | Serial drawings of coronal sections through one half of a human hypothalamus (*Homo sapiens*, specimen A18-05, 71 year old male) from the rostral aspect of the hypothalamus to the level of the mammillothalamic tract (**mmt**) showing the distribution of orexin-A immunopositive neurons. Part (a) is the most rostral section, and (g) the most caudal. The outlines of the architectonic regions were drawn using Nissl staining and orexin-A immunoreactive neurons marked on the drawings. Solid red dots represent orexinergic neurons of the main cluster (**Mc**), solid green dots represent orexinergic neurons of the zona incerta cluster (**Zic**), solid blue dots represent orexinergic neurons of the optic tract cluster (**OTc**), solid purple dots represent orexinergic neurons of the optic tract cluster extension (**OTce**), and solid black dots represent orexinergic neurons of the parvocellular cluster (**Pvc**). Each dot represents an individual neuron. The individual drawings comprising this figure (a–g) are approximately 1440 μm apart, and in each individual, drawing dorsal is to the top and medial to the left. See list for abbreviations.

expressing orexin, in humans or model animals, it is known that exposure to ethanol, heroin, and cocaine can selectively increase or decrease the number of neurons expressing orexin (McGregor et al. 2023, 2024). Thus, it is possible that the medications the patients, from which tissue specimens were obtained, were receiving prior to death may have reduced the number of neurons expressing orexin. It must also be mentioned that at any specific time, although a neuron may be capable of producing orexin, it may not be doing so. Thus, time of death may also play a role in the immunohistochemical revelation of orexinergic neurons, especially given that there is a clear circadian rhythm associated with orexinergic neurons (Marston et al. 2008).

Despite these potential methodological confounding factors, similar neuronal numbers for the total orexinergic neurons found in control humans have been reported in several previous, independently undertaken, studies (Thannickal, Moore et al. 2000, 2009; Fronczek et al. 2005, 2007, 2012; Valko et al. 2013; Table 2). Thus, with a reasonable degree of certainty, the significantly lower number of orexinergic neurons reported in humans is likely to be a reasonable reflection of reality. Although we generalize our results, we do so with caution, tempering our conclusions with awareness of these potential confounding factors.

### 4.2 | The Mc, Zic, and OTc in Primates

In mammals broadly, three orexinergic clusters are commonly identified, which include the Mc, Zic, and OTc (a nomenclature consolidated in Gravett et al. 2011, from earlier studies and

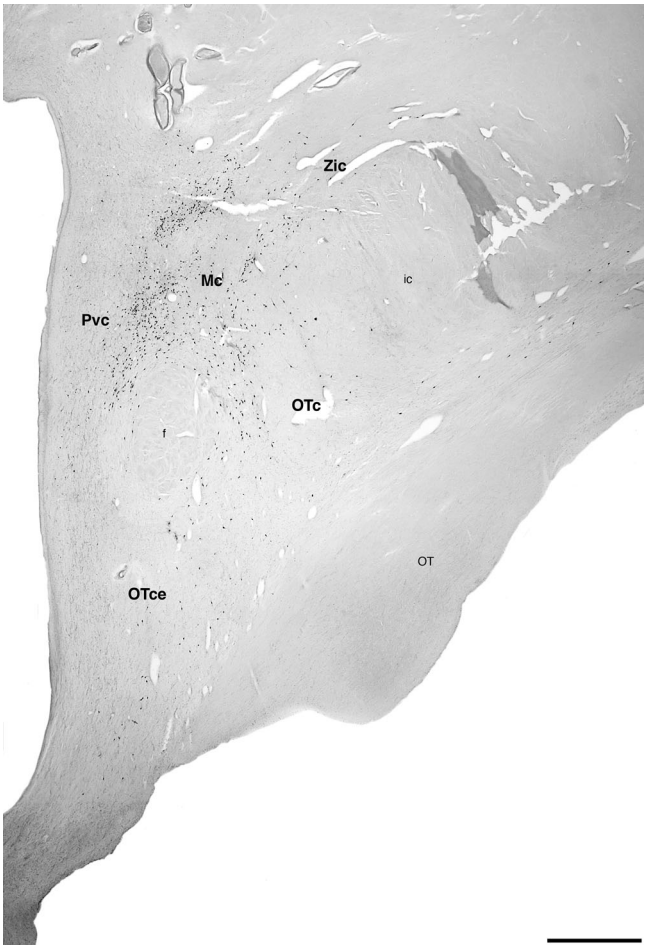


**FIGURE 11** | Low magnification photomicrograph of orexin-A immunopositive neurons in a human hypothalamus showing that the orexin-A immunopositive neurons could be subdivided into main (**Mc**), zona incerta (**Zic**), optic tract (**OTc**), optic tract extension (**OTce**), and parvocellular (**Pvc**) clusters. Dorsal is to the top and medial to the left. Scale bars = 2 mm. See list for abbreviations.

subsequently applied to many mammalian species, Oddes et al. 2023). These three clusters were proposed on the basis of both location within the hypothalamus and dendritic morphology. As described herein, the Mc, located in the perifornical region, comprises the majority of the orexinergic neurons, the dendrites of which show no specific preferred orientation. In contrast, smaller numbers of orexinergic neurons are found in the Zic and OTc, each of these clusters comprised neurons that exhibited specific preferred dendritic orientations (see Sections 3.1 and 3.3) located in the dorsomedial (adjacent to the zona incerta) and ventrolateral (adjacent to the optic tract) aspects of the hypothalamus. Although these three orexinergic clusters are commonly observed in mammals (Oddes et al. 2023), variations have been noted; for example, hamsters (McGranaghan and Piggins 2001) and microchiropteran bats (Kruger et al. 2010) lack the orexinergic neurons assigned to the OTc.

All primates, including humans, examined in the current study presented with the Mc, Zic, and OTc clusters. The primates are part of the Euarchontoglires, a mammalian superorder that is comprised of rodents, lagomorphs, tree shrews, colugos, and primates (Murphy et al. 2001). The orexinergic system has not been studied in colugos (the closest relatives of primates) but has been revealed in several rodent species (summarized in Oddes et al. 2023), a lagomorph, and a tree shrew (Calvey, Alagaili et al. 2015). All analyses of these species detail the Mc, Zic, and OTc clusters, just like the primates studied herein. Thus, across all primate species, the "core" clusters of the mammalian orexinergic system are found. It is therefore reasonable to conclude that the functional and connectional attributes of the "core mammalian" orexinergic system of primates, including humans, are likely to be consistent with that revealed in extensive detail in more commonly studied mammalian species.

### 4.3 | The OTce in the Hominoidea

In the lar gibbon and chimpanzee reinvestigated in the current study, and as reported previously (Williams et al. 2022), a low density of orexinergic neurons, with dorsoventrally oriented dendrites, was observed in the tuberal region of the hypothalamus. This neuronal cluster has been termed the OTce due to its topographical continuity with the OTc. The OTce was not previously noted in human studies (Thannickal, Moore et al. 2000, 2009; Fronczek et al. 2005, 2007, 2012; Valko et al. 2013), yet Krolewski et al. (2010) showed in humans, using in situ hybridization, that orexin mRNA is expressed in scattered neurons in the tuberal region of the hypothalamus, in the same location as we observed orexin-immunopositive neurons forming the OTce in the current reevaluation of the distribution of orexinergic neurons in the human. Thus, detailed mapping of the orexinergic neurons in humans and other hominoids, along with orexin mRNA (Krolewski et al. 2010), provide strong evidence for the OTce orexinergic cluster in Hominoidea and reveal that the parcellation of the orexinergic system is more complex than seen in the previously studied non-Hominoidea Euarchontoglires (also see Section 4.2).

The only other mammalian species in which similar neurons have been noted were the African and Asiatic lions and the southeast African cheetah, where these neurons have been designated as the supraoptic orexinergic cluster (Oddes et al. 2023). It is reasonable, with the currently available data, to consider the presence of these orexinergic neurons in Hominoidea and the big cats to be independent evolutionary events. Given the species in which the OTce orexinergic neurons have been observed (apes and big cats), it is highly unlikely that physiological recording of the activity of these neurons or determining their connectivity is likely to occur; thus, we can only speculate as to their potential functional correlates. The postsynaptic activity of orexin is generally excitatory (Bayer et al. 2004; Chrobok et al. 2017), chronologically relevant (Azeez et al. 2018), with the neurons generally having diffuse projections (Peyron et al. 1998), but there are a great deal of local projections within the hypothalamus. These theoretically additional OTce local projections may increase the influence of orexin in the tuberal region of the hypothalamus, a region involved in blood pressure control, water balance, thermoregulation, eating, reproduction, daily rhythms, stress and metabolic control, sleep, and arousal (e.g., Pop et al. 2018). It is possible that even the slightest augmentation of the local OTce orexinergic innervation on the supraoptic/tuberal regions of the hypothalamus may have a significant effect on the

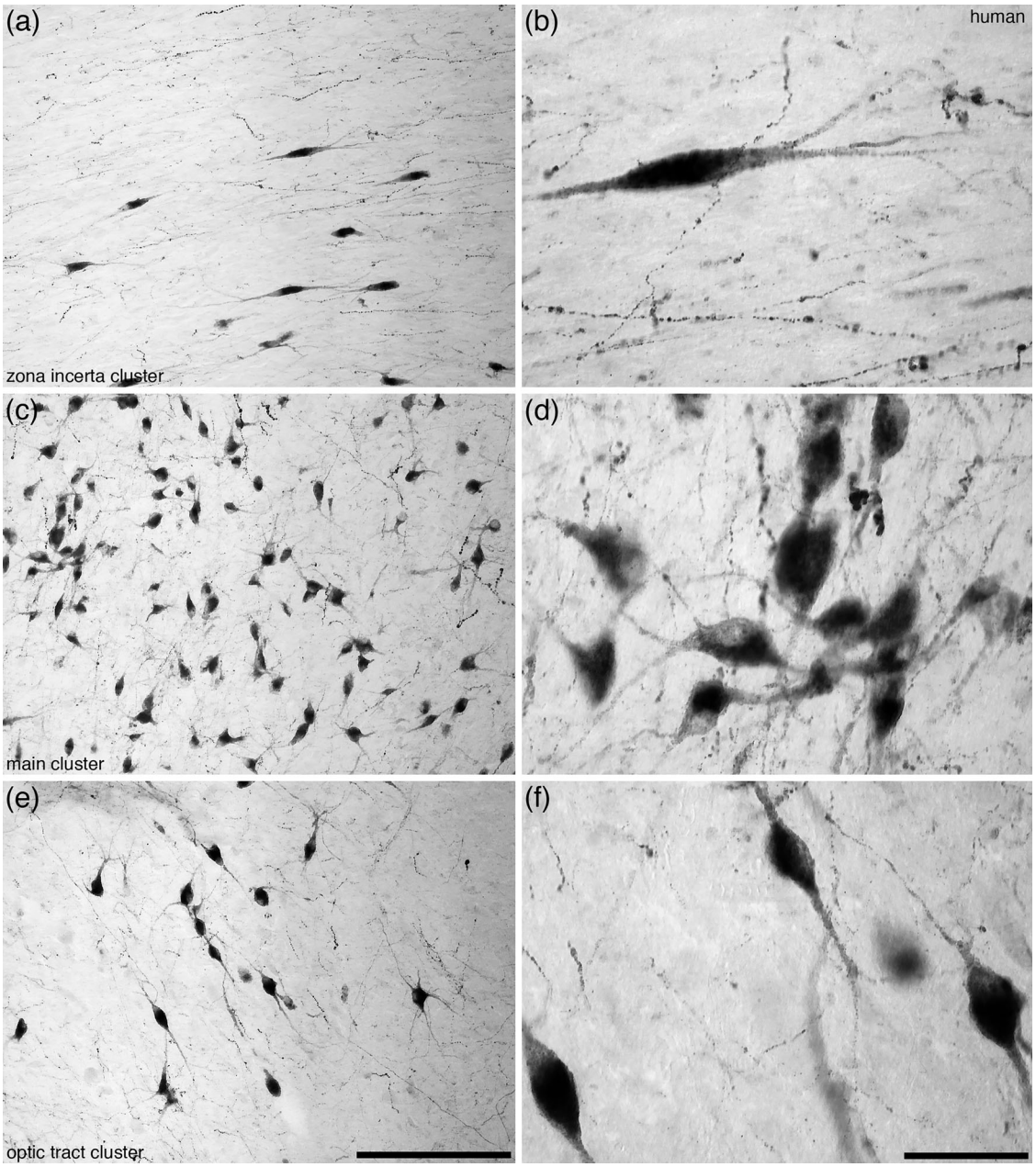


**FIGURE 12** | Moderate (a, c, e) and high (b, d, f) magnification photomicrographs of orexin-A immunopositive neurons in the hypothalamus of a human. Parts (a) and (b) depict orexinergic neurons of the zona incerta cluster, (c) and (d) orexinergic neurons of the main cluster, and (e) and (f) orexinergic neurons of the optic tract cluster. Note the preferred dendritic orientation in the zona incerta (a, b) and optic tract (e, f) clusters, whereas the neurons in the main cluster (c, d) show no preferred dendritic orientation. In all images, dorsal is to the top and medial to the left. Scale bar in (e) = 250 μm and applies to (a), (c), and (b). Scale bar in (f) = 50 μm and applies to (b), (d), and (f).

functionality of this portion of the hypothalamus, but at present, further speculation regarding the functional correlates of the activity of OTce orexinergic neurons requires further study.

### 4.4 | The Pvc of Humans

The presence of a dorsomedially located parvocellular orexinergic cluster (Pvc) in the human hypothalamus, as reported herein, is based on both the location and the relatively small soma volume of the neurons forming this cluster. Although the occasional small orexinergic neuron in this region of the hypothalamus has been noted in rodents (Nixon and Smale 2007), a distinct cluster of smaller orexinergic neurons in the dorsomedial hypothalamus was first described in the giraffe and harbor porpoise (Dell et al. 2012). This Pvc has since been observed in the minke whale (Dell, Karlsson et al. 2016), river hippopotamus (Dell, Patzke et al. 2016), Arabian oryx (Davimes et al. 2017), blue wildebeest (Malungo et al. 2020), African elephant (Maseko et al. 2013), Asiatic and African lions, southeast African cheetah (Oddes et al. 2023), and Perissodactyls (*pers. obs*. Ngwenya, Malungo, & Manger).

For the cetartiodactyls and perissodactyls, the Pvc is likely to be a neural trait inherited from the common ancestor of these

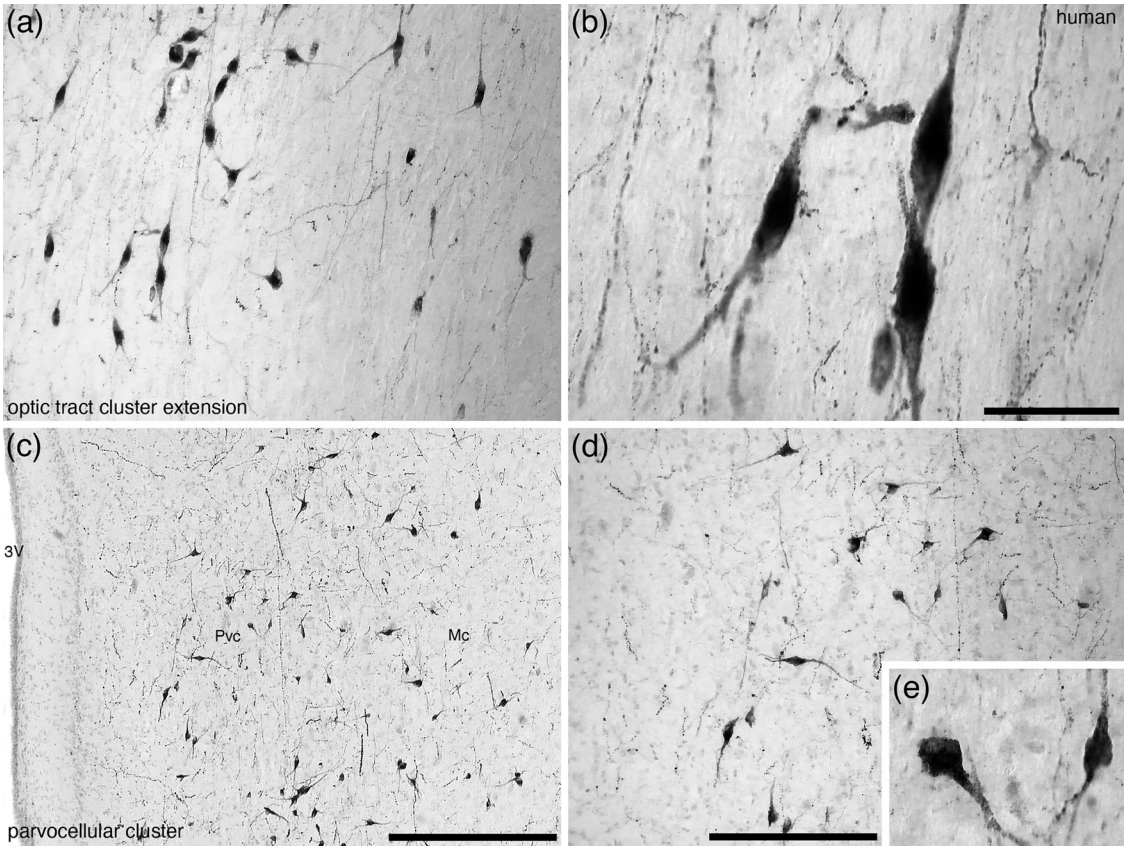


**FIGURE 13** | Low (c), moderate (a, d), and high (b, e) magnification photomicrographs of orexin-A immunopositive neurons in the hypothalamus of a human. Parts (a) and (b) depict orexinergic neurons of the optic tract cluster extension, a cluster of orexinergic neurons only observed in the Hominoidea primates (Williams et al. 2022). Note the consistent preferred dendritic orientation. (c–e) Orexinergic neurons of the parvocellular cluster (**Pvc**) that among primates have only been observed in the human. Note the lack of a preferred dendritic orientation of the neurons assigned to the **Pvc**, with the distinctly smaller sized soma compared to the other orexinergic clusters found in the human hypothalamus (e.g., the main cluster, **Mc**, shown in c). In all images, dorsal is to the top and medial to the left. Scale bar in (b) = 50 μm and applies to (a) and (e). Scale bar in (c) = 500 μm and applies to (c) only. Scale bar in (d) = 250 μm and applies to (b) and (d). **3 V**—third ventricle.

two lineages. In contrast, for the afrotherian African elephant and the carnivoran lions and cheetah, phylogenetically related species in which the orexinergic system has been described (Afrotheria: rock hyrax—Gravett et al. 2011; four-toed sengi, hottentot golden mole, giant otter shrew—Calvey et al. 2013; lesser hedgehog tenrec—Malungo et al. 2022; Carnivora: domestic dog—Thannickal, Nienhuis et al. 2000; domestic cat—Wagner et al. 2000; domestic ferret, banded mongoose—Pillay et al. 2017) did not reveal the presence of the Pvc. This indicates that the Pvc as a trait evolved either independently in these individual species or within species of a very restricted phylogenetic lineage (such as other species of the families Elephantidae or Panthera that are yet to be investigated). The presence of the Pvc in the human brain is unique neural trait among the primates that have been examined. Although the Pvc may only be present in *Homo sapiens* among the primates, it is possible that the Pvc is a shared neural trait of the species comprising the genus *Homo* (although the presence of this neural trait is unlikely to be revealed in the extinct species of the genus *Homo*).

To date, no physiological recording or connectional studies of the Pvc orexinergic neurons have been undertaken (likely due to the limited number of species in which this cluster has been found and the generally large size of these mammals); thus, we acknowledge that our discussion of Pvc neuronal function is purely speculative. Given the small size of these neurons, it is likely that they only send axonal projections locally, rather than diffusely throughout the brain (Peyron et al. 1998). It has been suggested that, as the Pvc neurons are found in mammals that tend to feed frequently for longer periods and tend to sleep less (cetartiodactyls, perissodactyls, and elephant), that these Pvc neurons play a role in driving both appetite and arousal, allowing time to consume the greater amount of food required in species that eat a high volume of low-caloric food (Malungo et al. 2020; but note the exception of cetaceans that eat a large volume of high-caloric food in response to their environment). In the lions and cheetah that eat infrequently and possibly have higher daily sleep times, it was suggested that the Pvc neurons may establish the heightened levels of arousal and hunger drive required for hunting (Oddes et al. 2023).

Of direct relevance to this line of reasoning are the findings that humans sleep the least of all primates (Samson 2021) and have the highest total energy expenditure of primates, thus requiring the greatest daily intake of food (Pontzer et al. 2016)—resembling the situation observed in artiodactyls, perissodactyls, and elephant, despite the fact that the caloric value of the food ingested by humans generally exceeds that of these herbivores.

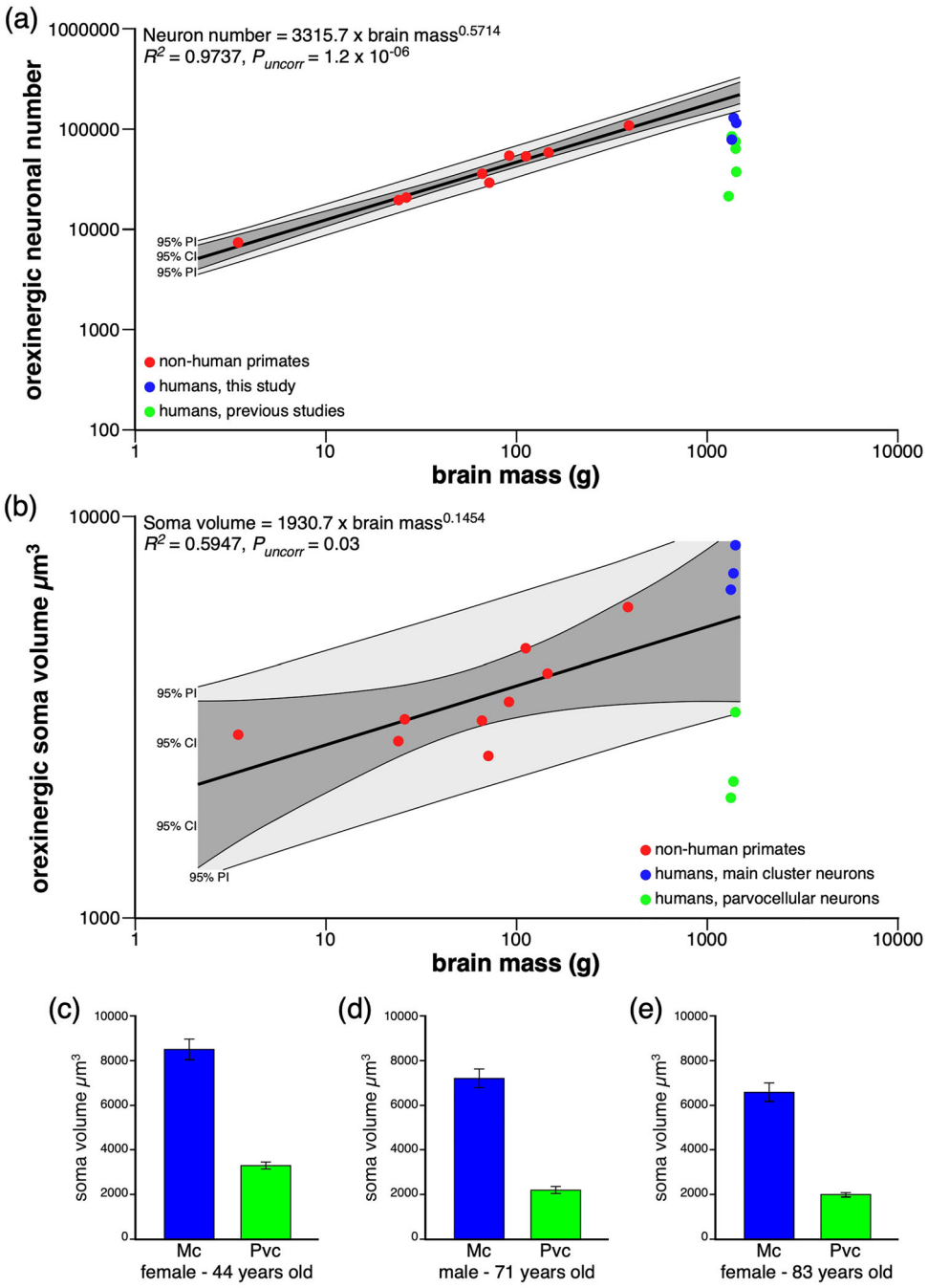


**FIGURE 14** | Graphs and bar plots of orexinergic neuronal numbers (a) and soma sizes (b–e) in the primates, including humans, analyzed in the current study (Table 2). (a) Regression plot of brain mass and orexinergic neuronal numbers in nonhuman primates (**red dots**) and humans (**blue dots**—data derived in this study; **green dots**—data from literature). Note that although there is a strongly statistically significant negative allometry in the nonhuman primates, the data for humans fall below the 95% confidence (**95% CI**) and prediction (**95% PI**) intervals for this regression. This indicates that humans have significantly lower orexinergic neuronal numbers than would be expected for a primate with human brain mass. (b) Regression plot of brain mass and orexinergic soma volume in nonhuman primates (**red dots**) and humans (**blue dots**—orexinergic neurons of the main cluster, **Mc**; **green dots**—orexinergic neurons of the parvocellular cluster, **Pvc**). Note that although there is a statistically significant negative allometry in the nonhuman primates, the data of **Mc** orexinergic soma volumes for human fall within the **95% CI** interval for this regression, having volumes that would be expected for a primate of human brain mass. In contrast, the data of **Pvc** orexinergic soma volumes for human fall below the **95% CI** and **95% PI** intervals for this regression, highlighting their small volume. (c, d, e) Bar plots of main cluster (**Mc**, **blue**) and parvocellular cluster (**Pvc**, **green**) average cell volumes, with standard deviation bars, in the 44-year-old female (c), 71-year-old male (d), and 83-year-old female (e), studied. The soma volumes of the **Pvc** are consistently statistically significantly smaller than those of the **Mc**.

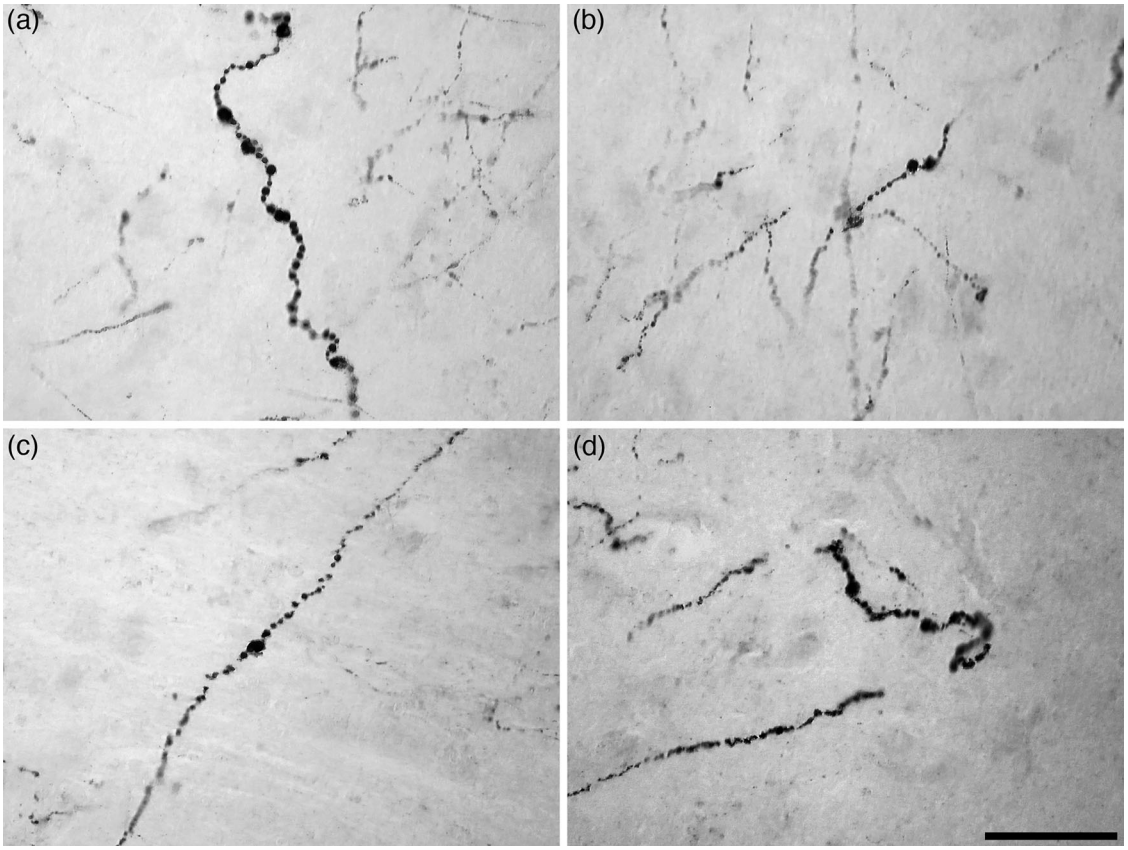


**FIGURE 15** | Photomicrographs showing the appearance of the orexinergic axonal terminals within the human hypothalamus. Note the "beaded" appearance of these orexinergic axonal terminals, with distinct larger and smaller boutons. Scale bar in (d) = 50 μm and applies to all.

The evolution of the larger, energetically expensive, brain in the *Homo* lineage (Manger et al. 2013) would require a greater daily caloric intake to maintain proper brain function. It is possible that the presence of Pvc orexinergic neurons in the *Homo* lineage facilitated the physiological states (arousal and hunger) required to maintain this relatively, and absolutely, larger brain in *Homo* species, including modern humans. Thus, it can be proposed that the Pvc orexinergic cluster observed in humans appeared at the emergence of the *Homo* lineage. This proposition is supported by the findings that the dorsomedial hypothalamus, where the Pvc is located, is involved in the monitoring of food availability in a circadian cycle (Gooley et al. 2006). Orexinergic neurons are known to be active in a circadian manner (Azeez et al. 2018) and regulate appetite, by stimulating food intake and repressing the neural circuits that control satiety (e.g., Kukkonen et al. 2002; Soya and Sakurai 2020; Zhang et al. 2013). We can then speculatively propose that the presence and activity of Pvc orexinergic neurons are an essential correlate of the energetics required for evolving a large brain in the *Homo* lineage.

The dorsomedial region of the hypothalamus is also involved in addiction (Zhang et al. 2018), with increased orexinergic neuronal numbers being observed in human addicts and animal models of addiction (Thannickal et al. 2018; James et al. 2019; Pantazis et al. 2020; McGregor et al. 2023, 2024). Addiction can be considered, in part, to be a dysregulation of the satiety neuronal circuits (Harricharan et al. 2017), which aligns with the findings that the orexinergic system represses the neural circuits controlling satiety (e.g., Kukkonen et al. 2002; Soya and Sakurai 2020; Zhang et al. 2013) and regulates cocaine self-administration (España et al. 2010) and relapse (Tung et al. 2016). It is then possible to propose that the presence of the Pvc orexinergic cluster in humans may play an important role in the human predisposition to addiction (Hunt et al. 2024), through the suppression of the hypothalamic portions of the satiety circuits (Ahima and Antwi 2008).

### 4.5 | Orexinergic Neuronal Numbers—The Human Paradox

While having a greater organizational complexity than other primates studied, the number of neurons comprising the orexinergic system in humans, with an average of approximately 74,300 (from all human data available in this study and previous literature, see Table 2), is about 36% of the number predicted based on the nonhuman primate regression for a primate brain with a mass of ~1363 g. Thus, the increased organizational complexity/specialization is paradoxically associated with relatively lower neuronal numbers. Although methodological differences (see Section 4.1) may partially account for this quantitative difference, the consistency of total orexinergic neuronal numbers across studies in humans from different laboratories (Thannickal et al. 2000; Fronczek et al. 2005, 2007, 2012; Valko et al. 2013) indicates that this is likely to be a real difference between humans and other primates.

As a corollary of this lower orexinergic neuronal number, we may predict that the density of orexinergic innervation throughout

the human brain is also relatively lower than other primates, as seen, for example, in cetaceans when compared to artiodactyls (Dell et al. 2015). However, if the human orexinergic systems were required to maintain an innervation density comparable to other primates, each human orexinergic soma would need to support a larger axon (in terms of volume, not diameter), providing the necessary increased volume of the terminal axonal field. An axon accounts for over 95% of the total volume of a neuron, reaching over 99.8% of neuronal volume in corticospinal neurons (Mihailoff and Haines 2018). In the current study, the somas of the human orexinergic neurons, averaging 7375 $\mu m^3$ (this excludes the Pvc soma), were the largest measured across the primates. Yet, humans do not have statistically larger soma than would be predicated based on soma size and brain mass in other primates. The regression analysis based on other primates indicates that humans should have soma volumes of 5514 $\mu m^3$, indicating that in humans the orexinergic soma are approximately 1860 $\mu m^3$ larger than would be expected for a primate with a brain mass of ~1363 g.

As a thought exercise, a rough mathematical estimation indicates that, if we assume that the axon represents 95% of the total neuronal volume, the axons of human orexinergic neurons (based only on a soma volume of 7375 $\mu m^3$, as we are unaware of data describing the proportion of neuronal volume occupied by dendrites, but in the case of bipolar orexinergic neurons, this should not be extremely large) should have a volume of around 140,000 $\mu m^3$. On the basis of the primate regression analysis, the soma volume of human orexinergic neurons is estimated to be 5514 $\mu m^3$, with a predicted axonal volume of 105,000 $\mu m^3$. Thus, in the human, it is possible that the larger orexinergic neurons support axons that are around 35,000 $\mu m^3$ larger (1.33 times) than expected based on data from other primates. Given that most of the axonal volume will be the terminal field arborization, the larger than predicted (although not statistically significant) human orexinergic neurons possibly support axons with terminal fields 1.33 times larger than expected. Can these possibly 1.33 times larger orexinergic axonal terminal fields in human maintain the same density of orexinergic innervation seen in nonhuman primates? If, as an example, we examine the neocortex in humans, it has been reported that the volume of the neocortical gray matter in humans is approximately 3.5 times larger than the chimpanzee (Stephan et al. 1981) and has 2.2 times as many neurons (7.4 billion neurons in the chimpanzee, Collins et al. 2016; 16.3 neurons in the human, Herculano-Houzel et al. 2015). Our findings indicate that the single chimpanzee studied, with 107,396 orexinergic neurons, has around 1.4 times the *average* number of orexinergic neurons found in humans (Table 2; note that the range for humans is 10,700–126,252. In our samples, there are two humans that have more orexinergic neurons than the single chimpanzee studied, but over 45 humans studied have fewer orexinergic neurons than the chimpanzee). In this sense, despite the increased soma volume and presumed 1.33 increase in axonal volume, in humans, it appears unlikely that these changes will provide the orexinergic innervation density matching that presumed to be present in other primates.

This line of reasoning necessarily implies that the density of the orexinergic axonal boutons in humans needs to be equivalent to that seen in other primates, but it is not known if this is the case. Examining the density (and size) of terminal orexinergic boutons in humans and other primates, as done previously in cetartiodactyls (Dell et al. 2015), would be instructive in terms of understanding the potential mechanism by which, if indeed it is needed, the human brain maintains an orexinergic innervation density like that of other primates. Alternatively, it may reveal that orexinergic innervation in human brains is lower than in other primates (and possibly other mammals, particularly those commonly used in translational research), with such a finding requiring a reevaluation of the translation of results related to the orexinergic system in model animals to humans.

### 4.6 | Orexinergic Axonal Terminal Bouton Morphology

In previously studied species, including Cetartiodactyla (Dell et al. 2015), lar gibbon, chimpanzee (Williams et al. 2022), lions, cheetah (Oddes et al. 2023), and several species of larger-brained birds (Mazengenya et al. 2024), it was noted that the orexinergic terminal axons contained two bouton types, large and small. As orexin produces a postsynaptic excitatory effect (Song et al. 2006; Yan et al. 2012), the two bouton sizes suggest that orexin can act through chemical synapses formed with the larger boutons and through volume transmission (Fuxe et al. 2010) with the smaller boutons. Indeed, orexin has been shown to be able to communicate through both mechanisms, with volume transmission mechanism producing a sustained modulatory activation of recipient neurons, whereas that produced by the synaptic mechanism is transitory but specific (Del Cid-Pellitero and Garzón 2011). The consistency of this finding across a broad range of species, including humans, indicates that these two modes of orexinergic communication are likely to be similar across all vertebrates. This is an important aspect of the neurophysiology of orexinergic communication that requires a more detailed understanding, especially in terms of the potential effects of therapeutics targeting the orexinergic system—such therapeutics might have unintended actions.

#### Author Contributions

Illke B. Malungo, Ayanda Ngwenya, Jerome M. Siegel, and Paul R. Manger conceptualized the study. Thomas C. Thannickal and Jerome M. Siegel provided the human material used in this study. Mads F. Bertelsen obtained and prepared the nonhuman primate brains used in this study. Illke B. Malungo, Ayanda Ngwenya, Thomas C. Thannickal, Jerome M. Siegel, Muhammad A. Spocter, and Paul R. Manger performed the staining and analysis. Illke B. Malungo and Paul R. Manger wrote the initial draft of the manuscript, and all authors contributed to the editing and improvement of the early drafts of the manuscript. All authors had full access to all data in the study and take responsibility for the integrity of the data and the accuracy of the data analysis.

#### Acknowledgments

We thank Dr. João Paulo Coimbra for his assistance with the acquisition of some of the primate brains used in this study.

#### Ethics Statement

The primates used in this study were treated according to the guidelines of the University of Witwatersrand Animal Ethics Committee (Clearance number 2017/010/73/O), which correspond with those of the NIH for care and use of animals in scientific experimentation.

## Conflicts of Interest

The authors declare no conflicts of interest.

## Data Availability Statement

Data have not been shared due to this study being based on histological sections.

## Peer Review

The peer review history for this article is available at https://publons.com/publon/10.1002/cne.70032.

## References


Ahima, R. S., and D. A. Antwi. 2008. "Brain Regulation of Appetite and Satiety." *Endocrinology and Metabolism Clinics* 37: 811–823. https://doi.org/10.1016/j.ecl.2008.08.005.

Arnold, C., L. J. Matthews, and C. L. Nunn. 2010. "The 10kTrees Website: A New Online Resource for Primate Phylogeny." *Evolutionary Anthropology* 19: 114–118. https://doi.org/10.1002/evan.20251.

Azeez, I. A., F. del Gallo, L. Cristino, and M. Bentivoglio. 2018. "Daily Fluctuation of Orexin Neuron Activity and Wiring: The Challenge of "Chronoconnectivity"." *Frontiers in Pharmacology* 9: 1061. https://doi.org/10.3389/fphar.2018.01061.

Bayer, L., M. Serafin, E. Eggerman, et al. 2004. "Exclusive Postsynaptic Action of Hypocretin-Orexin on Sublayer 6b Cortical Neurons." *Journal of Neuroscience* 24: 6760–6764. https://doi.org/10.1523/JNEUROSCI.1783-04.2004.

Bertelsen, M. F. 2018. "Issues Surrounding Surplus Animals in Zoos." In *Fowler's Zoo and Wild Animals Medicine, Current Therapy*, edited by R. E. Miller N. Lamberski, and P. Calle, 134–137. Elsevier.

Blouin, A. M., I. Fried, C. L. Wilson, et al. 2013. "Human Hypocretin and Melanin-Concentrating Hormone Levels Are Linked to Emotion and Social Interaction." *Nature Communications* 4: 1547. https://doi.org/10.1038/ncomms2461.

Calvey, T., A. N. Alagaili, M. F. Bertelsen, A. Bhagwandin, J. D. Pettigrew, and P. R. Manger. 2015. "Nuclear Organisation of Some Immunohistochemically Identifiable Neural Systems in Two Species of the Euarchontoglires: A Lagomorph, *Lepus capensis*, and a Scandentia, *Tupaia Belangeri*." *Journal of Chemical Neuroanatomy* 70: 1–19. https://doi.org/10.1016/j.jchemneu.2015.10.007.

Calvey, T., N. Patzke, C. Kaswera, E. Gilissen, N. C. Bennett, and P. R. Manger. 2013. "Nuclear Organisation of Some Immunohistochemically Identifiable Neural Systems in Three Afrotherian Species—*Potomogale velox*, *Amblysomus hottentotus* and *Petrodromus tetradactylus*." *Journal of Chemical Neuroanatomy* 50–51: 48–65. https://doi.org/10.1016/j.jchemneu.2013.01.002.

Calvey, T., N. Patzke, C. Kaswera-Kyamakya, et al. 2015. "Organization of Cholinergic, Catecholaminergic, Serotonergic and Orexinergic Nuclei in Three Strepsirrhine Primates: *Galago demidoff*, *Perodicticus potto* and *Lemur catta*." *Journal of Chemical Neuroanatomy* 20: 42–57. https://doi.org/10.1016/j.jchemneu.2015.10.007.

Chrobok, L., K. Palus-Chramiec, A. Chrzanowska, M. Kepczynski, and M. H. Lewandowski. 2017. "Multiple Excitatory Actions of Orexins Upon Thalamo-Cortical Neurons in Dorsal Lateral Geniculate Nucleus—Implications for Vision Modulation by Arousal." *Scientific Reports* 7: 7713. https://doi.org/10.1038/s41598-017-08202-8.

Collins, C. E., E. C. Turner, E. K. Sawyer, et al. 2016. "Cortical Cell and Neuron Density Estimates in One Chimpanzee Hemisphere." *Proceedings of the National Academy of Science USA* 113: 740–745. https://doi.org/10.1073/pnas.1524208113.

Davimes, J. G., A. N. Alagaili, N. C. Bennett, et al. 2017. "Neurochemical Organization and Morphology of the Sleep Related Nuclei in the Brain of the Arabian Oryx, *Oryx leucoryx*." *Journal of Chemical Neuroanatomy* 81: 53–70. https://doi.org/10.1016/j.jchemneu.2017.02.002.

del Cid-Pellitero, E., and M. Garzón. 2011. "Hypocretin1/Orexin-A Immunoreactive Axons Form Few Synaptic Contacts on Rat Ventral Tegmental Area Neurons That Project to the Medial Prefrontal Cortex." *BMC Neuroscience* 7: 105. https://doi.org/10.1186/1471-2202-15-105.

Dell, L. A., K. Æ. Karlsson, N. Patzke, M. A. Spocter, J. M. Siegel, and P. R. Manger. 2016. "Organization of the Sleep-Related Neural Systems in the Brain of the Minke Whale (*Balaenoptera acutorostrata*)." *Journal of Comparative Neurology* 524: 2018–2035. https://doi.org/10.1002/cne.23931.

Dell, L. A., N. Patzke, A. Bhagwandin, et al. 2012. "Organization and Number of Orexinergic Neurons in the Hypothalamus of Two Species of Cetartiodactyla: A Comparison of Giraffe (*Giraffe camelopardalis*) and Harbour Porpoise (*Phocoena phocoena*)." *Journal of Chemical Neuroanatomy* 44: 98–109. https://doi.org/10.1016/j/jchemneu.2012.06.001.

Dell, L. A., N. Patzke, M. A. Spocter, M. F. Bertelsen, J. M. Siegel, and P. R. Manger. 2016. "Organization of the Sleep-Related Neural Systems in the Brain of the River Hippopotamus (*Hippopotamus amphibius*)." *Journal of Comparative Neurology* 524: 2036–2058. https://doi.org/10.1002/cne.23930.

Dell, L. A., M. A. Spocter, N. Patzke, et al. 2015. "Orexinergic Bouton Density Is Lower in the Cerebral Cortex of Cetaceans Compared to Artiodactyls." *Journal of Chemical Neuroanatomy* 68: 61–78. https://doi.org/10.1016/j.jchemneu.2015.07.007.

Downs, J. L., M. R. Dunn, E. Borok, et al. 2007. "Orexin Neuronal Changes in the Locus Coeruleus of the Aging Rhesus Macaque." *Neurobiology of Aging* 28: 1286–1295. https://doi.org/10.1016/j.neurobiolaging.2006.05.025.

Elias, C. F., C. B. Saper, E. Maratos-Flier, et al. 1998. "Chemically Defined Projections Linking the Mediobasal Hypothalamus and the Lateral Hypothalamic Area." *Journal of Comparative Neurology* 402: 442–459. https://doi.org/10.1002/(SICI)1096-9861(19981228)402:4⟨442::AID-CNE2⟩3.0.CO;2-R.

España, R. A., E. B. Oleson, J. L. Locke, B. R. Brookshire, D. C. S. Roberts, and S. R. Jones. 2010. "The Hypocretin-Orexin System Regulates Cocaine Self-Administration via Actions on the Mesolimbic Dopamine System." *European Journal of Neuroscience* 31: 336–348. https://doi.org/10.1111/j.1460-9568.2009.07065.x.

Fronczek, R., G. J. Lammers, R. Balesar, U. A. Unmehopa, and D. F. Swaab. 2005. "The Number of Hypothalamic Hypocretin (Orexin) Neurons Is Not Affected in Prader-Willi Syndrome." *Journal of Clinical Endocrinology & Metabolism* 90: 5466–5470. https://doi.org/10.1210/jc.2005-0296.

Fronczek, R., S. Overeem, S. Y. Y. Lee, et al. 2007. "Hypocretin (Orexin) Loss in Parkinson's Disease." *Brain* 130: 1577–1585. https://doi.org/10.1093/brain/awm090.

Fronczek, R., S. van Geest, M. Frölich, et al. 2012. "Hypocretin (Orexin) Loss in Alzheimer's Disease." *Neurobiology of Aging* 33: 1642–1650. https://doi.org/10.1016/j.neurobiolaging.2011.03.014.

Fuxe, K., A. B. Dahlstrom, G. Jonsson, et al. 2010. "The Discovery of Central Monoamine Neurons Gave Volume Transmission to the Wired Brain." *Progress in Neurobiology* 90: 820–900. https://doi.org/10.1016/j.pneurobio.2009.10.012.

Gooley, J. J., A. Schomer, and C. B. Saper. 2006. "The Dorsomedial Hypothalamic Nucleus Is Critical for the Expression of Food-Entrainable Circadian Rhythms." *Nature Neuroscience* 9: 398–407. https://doi.org/10.1038/mm1651.

Gravett, N., A. Bhagwandin, K. Fuxe, and P. R. Manger. 2011. "Distribution of Orexin—A Immunoreactive Neurons and Their Terminal Networks in the Brain of the Rock Hyrax, *Procavia capensis*." *Journal of Chemical Neuroanatomy* 41: 86–96. https://doi.org/10.1016/j.jchemneu.2010.11.005.

Gundersen, H. J. 1988. "The Nucleator." *Journal of Microscopy—Oxford* 151: 3–21. https://doi.org/10.1111/j.1365-2818.1988.tb04609.x.

Harricharan, R., O. Abboussi, and W. M. U. Daniels. 2017. "Chapter 3—Addiction: A Dysregulation of Satiety and Inflammatory Processes." *Progress in Brain Research* 235: 65–91. https://doi.org/10.1016/bs.pbr.2017.07.012.

Herculano-Houzel, S., K. Catania, P. R. Manger, and J. H. Kaas. 2015. "Mammalian Brains Are Made of These: A Dataset of the Numbers and Densities of Neuronal and Nonneuronal Cells in the Brain of Glires, Primates, Scandentia, Eulipotyphlans, Afrotherians and Artiodactyls, and Their Relationship With Body Mass." *Brain, Behavior and Evolution* 86: 145–163. https://doi.org/10.1159/000437413.

Hunt, A., G. P. Merola, T. Carpenter, and A. V. Jaeggi. 2024. "Evolutionary Perspectives on Substance and Behavioural Addictions: Distinct and Shared Pathways to Understanding, Prediction and Prevention." *Neuroscience and Biobehavioral Reviews* 159: 105603. https://doi.org/10.1016/j.neubiorev.2024.105603.

Inutsuka, A., and A. Yamanaka. 2013. "The Regulation of Sleep and Wakefulness by the Hypothalamic Neuropeptide Orexin/Hypocretin." *Nagoya Journal of Medical Science* 75: 29–36.

James, M. H., C. M. Stopper, B. A. Zimmer, N. E. Koll, H. E. Bowrey, and G. Aston-Jones. 2019. "Increased Number and Activity of a Lateral Subpopulation of Hypothalamic Orexin/Hypocretin Neurons Underlies the Expression of an Addicted State in Rats." *Biological Psychiatry* 85: 925–935. https://doi.org/10.1016/j.biopsych.2018.07.022.

Krolewski, D. M., A. Medina, I. A. Kerman, et al. 2010. "Expression Patterns of Corticotropin-Releasing Factor, Arginine Vasopressin, Histidine Decarboxylase, Melanin-Concentrating Hormone, and Orexin Genes in the Human Hypothalamus." *Journal of Comparative Neurology* 518: 4591–4611. https://doi.org/10.1002/cne.22480.

Kruger, J.-L., L.-A. Dell, J. D. Pettigrew, and P. R. Manger. 2010. "Cellular Location and Major Terminal Networks of the Orexinergic System in the Brains of Five Microchiropteran Species." *Journal of Chemical Neuroanatomy* 40: 256–262. https://doi.org/10.1016/j.jchemneu.2010.07.004.

Kukkonen, J. P., T. Holmqvist, S. Ammoun, and K. E. O. Åkerman. 2002. "Functions of the Orexinergic/Hypocretinergic System." *American Journal of Physiology—Cell Physiology* 283: C1567–C1591. https://doi.org/10.1152/ajpcell.00055.2002.

Luna, S. L., D. I. Brown, D. H. Eghlidi, S. G. Kohama, and H. F. Urbanski. 2017. "Locomotor Activity and the Expression of Orexin A and Orexin B in Aged Female Rhesus Macaques." *Neurobiology of Aging* 50: 1–4. https://doi.org/10.1016/j.neuroioaging.2016.10.016.

Malungo, I. B., N. Gravett, A. Bhagwandin, J. G. Davimes, and P. R. Manger. 2020. "A Preliminary Description of the Sleep-Related Neural Systems in the Brain of the Blue Wildebeest, *Connochaetes taurinus*." *Anatomical Record* 303: 1977–1997. https://doi.org/10.1002/ar.24265.

Malungo, I. B., R. Mokale, M. F. Bertelsen, and P. R. Manger. 2022. "Cholinergic, Catecholaminergic, Serotonergic, and Orexinergic Neuronal Populations in the Brain of the Lesser Hedgehog Tenrec (*Echinops telfairi*)." *Anatomical Record* 306: 844–878. https://doi.org/10.1002/ar.25092.

Manger, P. R., P. Pillay, B. C. Maseko, et al. 2009. "Acquisition of Brains From the African Elephant (*Loxodonta africana*): Perfusion-Fixation and Dissection." *Journal of Neuroscience Methods* 179: 16–21. https://doi.org/10.1016/j/jneumeth.2009.01.001.

Manger, P. R., M. A. Spocter, and N. Patzke. 2013. "The Evolutions of Large Brain Size in Mammals: The 'Over-700-Gram Club Quartet'." *Brain, Behavior and Evolution* 82: 68–78. https://doi.org/10.1159/000352056.

Marston, O. J., R. H. Williams, M. M. Canal, R. E. Samuels, N. Upton, and H. D. Piggins. 2008. "Circadian and Dark-Pulse Activation of Orexin/Hypocretin Neurons." *Molecular Brain* 1: 19. https://doi.org/10.1186/1756-6606-1-19.

Maseko, B. C., N. Patzke, K. Fuxe, and P. R. Manger. 2013. "Architectural Organization of the African Elephant Diencephalon and Brainstem." *Brain, Behavior and Evolution* 82: 83–128. https://doi.org/10.1159/000352004.

Mazengenya, P., M. A. Spocter, and P. R. Manger. 2024. "Nuclear Parcellation and Numbers of Orexinergic Neurons in Five Species of Larger Brained Birds." *Journal of Comparative Neurology* 532: e25602. https://doi.org/10.1002/cne.25432.

McGranaghan, P. A., and H. D. Piggins. 2001. "Orexin-A-Like Immunoreactivity in the Hypothalamus and Thalamus of the Syrian Hamster (*Mesocricetus auratus*) and Siberian Hamster (*Phodopus sungorus*), With Special Reference to Circadian Structures." *Brain Research* 904: 234–244. https://doi.org/10.1016/s0006-8993(01)02463-5.

McGregor, R., A. Matzeu, T. C. Thannickal, et al. 2023. "Sensitivity of Hypocretin System to Chronic Alcohol Exposure: A Human and Animal Study." *Neuroscience* 522: 1–10. https://doi.org/10.1016/j.neuroscience.2023.04.018.

McGregor, R., M.-F. Wu, G. Barber, L. Ramanathan, and J. M. Siegel. 2011. "Highly Specific Role of Hypocretin (Orexin) Neurons: Differential Activation as a Function of Diurnal Phase, Operant Reinforcement vs. Operant Avoidance and Light Level." *Journal of Neuroscience* 31: 15455–15467. https://doi.org/10.1523/JNEUROSCI.4017-11.2011.

McGregor, R., M.-F. Wu, T. C. Thannickal, and J. M. Siegel. 2024. "Opiate Anticipation, Opiate Induced Anatomical Changes in Hypocretin (Hcrt, Orexin) Neurons and Opiate Induced Microglial Activation are Blocked by the Dual Hcrt Receptor Antagonist Suvorexant, While Opiate Analgesia is Maintained." bioR$\chi$iv. https://doi.org/10.1101/2023.09.22.559044.

Mihailoff, G. A., and D. E. Haines. 2018. "Chapter 2—The Cell Biology of Neurons and Glia." In *Fundamental Neuroscience for Basic and Clinical Applications*, edited by D. E. Haines and G. A. Mihailoff, 4th ed., 15–33. Elsevier. https://doi.org/10.1016/B978-0-323-39632-5.00002-5.

Moore, R. Y., E. A. Abrahamson, and A. van den Pol. 2001. "The Hypocretin Neuron System: An Arousal System in the Human Brain." *Archives Italiennes Biologie* 139: 195–205.

Murphy, W. J., E. Eizirik, S. J. O'Brien, et al. 2001. "Resolution of the Early Placental Mammal Radiation Using Bayesian Phylogenetics." *Science* 294: 2348–2351. https://doi.org/10.1126/science.1067179.

Nixon, J. P., and L. Smale. 2007. "A Comparative Analysis of the Distribution of Immunoreactive Orexin A and B in the Brains of Nocturnal and Diurnal Rodents." *Behavioral and Brain Functions* 3: 28. https://doi.org/10.1186/1744-9081-3-28.

Oddes, D., A. Ngwenya, I. B. Malungo, et al. 2023. "Orexinergic Neurons in the Hypothalamic of an Asiatic Lion, an African Lion, and a Southeast African Cheetah." *Journal of Comparative Neurology* 531: 366–389. https://doi.org/10.1002/cne.25432.

Orme, C. D. L., R. P. Freckleton, G. H. Thomas, T. Petzoldt, S. A. Fritz, and N. J. B. Isaac. 2013. "Caper: Comparative Analyses of Phylogenetics and Evolution in R." *Methods in Ecology and Evolution* 3: 145–151.

Pantazis, C. B., M. H. James, B. S. Bentzley, and G. Aston-Jones. 2020. "The Number of Lateral Hypothalamus Orexin/Hypocretin Neurons Contributes to Individual Differences in Cocaine Demand." *Addiction Biology* 25: e12795. https://doi.org/10.1111/adb.12795.

Peyron, C., D. K. Tighe, A. N. van den Pol, et al. 1998. "Neurons Containing Hypocretin (Orexin) Project to Multiple Neuronal Systems." *Journal of Neuroscience* 18: 9996–10015. https://doi.org/10.1523/JNEUROSCI.18-23-09996.1998.

Pillay, S., A. Bhagwandin, M. F. Bertelsen, et al. 2017. "Regional Distribution of Cholinergic, Catecholaminergic, Serotonergic and Orexinergic Neurons in the Brain of Two Carnivore Species: The Feliform Banded Mongoose (*Mungos mungo*) and the Caniform Domestic Ferret (*Mustela putorius furo*)." *Journal of Chemical Neuroanatomy* 82: 12–28. https://doi.org/10.1016/j.jchemneu.2017.04.001.

Pontzer, H., M. H. Brown, D. A. Raichlen, et al. 2016. "Metabolic Acceleration and the Evolution of Human Brain Size and Life History." *Nature* 533: 390–392. https://doi.org/10.1038/nature17654.

Pop, M. G., C. Crivii, and I. Opincariu. 2018. “Chapter 1. Anatomy and Function of the Hypothalamus.” In *The Hypothalamus in Health and Disease*, edited by S. Baloyannis and J. Gordeladze, 3–14. IntechOpen. https://doi.org/10.5772/intechopen.80728.

Samson, D. R. 2021. “The Human Sleep Paradox: The Unexpected Sleeping Habits of Homo Sapiens.” *Annual Review of Anthropology* 50: 259–274. https://doi.org/10.1146/annurev-anthro-010220-075523.

Siegel, J. M. 2022. “Sleep Function: An Evolutionary Perspective.” *Lancet Neurology* 21: 937–946. https://doi.org/10.1016/S1474-4422(22)00210-1.

Smaers, J. B., and F. J. Rohlf. 2016. “Testing Species’ Deviation From Allometric Predictions Using the Phylogenetic Regression.” *Evolution; International Journal of Organic Evolution* 70: 1145–1149. https://doi.org/10.1111/evo.12910.

Song, C., X. Chen, J. Xia, Z. Yu, and Z. Hu. 2006. “Modulatory Effects of Hypocretin-1/Orexin-A With Glutamate and γ-Aminobutyric Acid on Freshly Isolated Pyramidal Neurons From the Rat Prefrontal Cortex.” *Neuroscience Letters* 399: 101–105. https://doi.org/10.1016/j.neulet.2006.01.065.

Soya, S., and T. Sakurai. 2020. “Evolution of Orexin Neuropeptide System: Structure and Function.” *Frontiers in Neuroscience* 14: 691. https://doi.org/10.3389/fnins.2020.00691.

Stephan, H., H. Frahm, and G. Baron. 1981. “New and Revised Data on Volumes of Brain Structures in Insectivores and Primates.” *Folia Primatologica* 35: 1–29. https://doi.org/10.1159/000155963.

Thannickal, T. C., J. John, L. Shan, et al. 2018. “Opiates Increase the Number of Hypocretin-Producing Cells in Mouse and Human Brain and Reverse Cataplexy in a Mouse Model of Narcolepsy.” *Science Translational Medicine* 447: eaao4953. https://doi.org/10.1126/scitranslmed.aao4953.

Thannickal, T. C., R. Y. Moore, R. Nienhuis, et al. 2000. “Reduced Number of Hypocretin Neurons in Human Narcolepsy.” *Neuron* 27: 469–474. https://doi.org/10.1016/s0896-6273(00)00058-1.

Thannickal, T. C., R. Neinhuis, and J. M. Siegel. 2009. “Localized Loss of Hypocretin (Orexin) Cells in Narcolepsy Without Cataplexy.” *Sleep* 32: 993–998. https://doi.org/10.1093/sleep/32.8.993.

Thannickal, T. C., R. Nienhuis, L. Ramanathan, et al. 2000. “Preservation of Hypocretin Neurons in Genetically Narcoleptic Dogs.” *Sleep* 23: A296–A296.

Tsujino, N., and T. Sakurai. 2009. “Orexin/Hypocretin: A Neuropeptide at the Interfaces of Sleep, Energy Homeostasis, and Reward System.” *Pharmacological Reviews* 61: 162–176. https://doi.org/10.1124/pr.109.001321.

Tung, L.-W., G.-L. Lu, Y.-H. Lee, et al. 2016. “Orexins Contribute to Restraint Stress-Induced Cocaine Relapse by Endocannabinoid-Mediated Disinhibition of Dopaminergic Neurons.” *Nature Communications* 7: 12199. https://doi.org/10.1038/ncomms12199.

Valko, P. O., Y. V. Gavrilov, M. Yamamoto, et al. 2013. “Increase of Histaminergic Tuberomammillary Neurons in Narcolepsy.” *Annals of Neurology* 74: 794–804. https://doi.org/10.1002/ana.24019.

Volkhoff, H. 2012. “Sleep and Orexins in Nonmammalian Vertebrates.” *Vitamins and Hormones* 89: 315–319. https://doi.org/10.1016/B978-0-12-394623-2.00017-2.

Wagner, D., R. Salin-Pascual, M. A. Greco, and P. J. Shiromani. 2000. “Distribution of Hypocretin-Containing Neurons in the Lateral Hypothalamus and c-Fos-Immunoreactive Neurons in the VLPO.” *Sleep Research Online* 3: 35–42.

West, M. J., L. Slomianka, and H. J. Gundersen. 1991. “Unbiased Stereological Estimation of the Total Number of Neurons in the Subdivisions of the Rat Hippocampus Using the Optical Fractionator.” *Anatomical Record* 231: 482–497. https://doi.org/10.1002/ar.1092310411.

Williams, V. M., A. Bhagwandin, J. Swiegers, et al. 2022. “Nuclear Organization of Orexinergic Neurons in the Hypothalamus of a Lar Gibbon and a Chimpanzee.” *Anatomical Record* 305: 1459–1475. https://doi.org/10.1002/ar24775.

Yan, J., C. He, J. Xia, D. Zhang, and Z. Hu. 2012. “Orexin—A Excites Pyramidal Neurons in Layer 2/3 of the Prefrontal Cortex.” *Neuroscience Letters* 520: 92–97. https://doi.org/10.1016/j.neulet.2012.05.038.

Zhang, S., S. Zhornitsky, G. A. Angarita, and C.-R. Li. 2018. “Hypothalamic Response to Cocaine Cures and Cocaine Addiction Severity.” *Addiction Biology* 25: e12682. https://doi.org/10.1111/adb.12682.

Zhang, X. Y., L. Yu, Q. X. Zhuang, J. N. Zhu, and J. J. Wang. 2013. “Central Functions of the Orexinergic System.” *Neuroscience Bulletin* 29: 355–365. https://doi.org/10.1007/s12264-012-1297-4.